Supporting Information

Cleavage of Acyclic Diaminocarbene Ligands at an Iridium(III) Center. Recognition of a New Reactivity Mode for Carbene Ligands

Mikhail A. Kinzhalov,*[,a] Anzhelika A. Eremina,[a] Andrey S. Smirnov,[a] Vitalii V. Suslonov,[a] Vadim Yu. Kukushkin,[a] Konstantin V. Luzyanin*[,a,b]

[a]Saint Petersburg State University, 7/9 Universitetskaya Nab., Saint Petersburg, 199034 Russia;

[b]Department of Chemistry, University of Liverpool, Crown Street, Liverpool L69 7ZD, United Kingdom

Table of Contents

1. Characterization of isocyanide and diaminocarbene complexes

1.1. Characterization of complexes [3a–b](OTf)

Complexes [**3a**–**d**](OTf) were characterized by elemental analyses (C, H, N), molar conductivity measurements, TG/DTA, high resolution ESI$^+$-MS, IR, 1D (^{1}H, ^{13}C{^{1}H}, ^{19}F{^{1}H}) and 2D (^{1}H,^{1}H COSY, ^{1}H,^{13}C-HMQC/^{1}H,^{13}C-HSQC, ^{1}H,^{13}C-HMBC) NMR spectroscopy. Complexes [**3a**–**d**](OTf) gave satisfactory CHN microanalyses, that are consistent with the proposed formulae. The values of molar conductivities of [**3a**–**d**](OTf) in MeCN (137–148 Ohm^{-1}cm^{-1}mol^{-1}) agree with the typical range for 1:1 electrolytes (120–160 Ohm^{-1}cm^{-1}mol^{-1} in MeCN[1]). The HRESI$^+$-MS of [**3a**–**d**](OTf) exhibit sets of peaks with the characteristic isotopic distribution due to [M – OTf]$^+$ ions. The IR spectra of [**3a**–**d**](OTf) contain two strong ν(C≡N) bands in the 2145–2156 cm^{-1} and 2173–2184 cm^{-1} ranges, that is consistent with the *cis* placement of the two isocyanide ligands. Increase of the CN stretching vibration frequency on going from the uncomplexed (2129–2140 cm^{-1}; Table S1, ESI) to the coordinated isocyanides [**3a–d**](OTf) indicates the more pronounced electrophilic character of the C atom of ligated isocyanide and its higher susceptibility to the nucleophilic attack.[2] Herein, a small $\Delta\nu = \nu(C{\equiv}N)_{coord} - \nu(C{\equiv}N)_{free}$ of *ca*. 30 cm^{-1} for [**3a**−**c**](OTf) (5 cm^{-1} for [**3d**](OTf)) indicates a limited electrophilic activation of coordinated isocyanides towards reaction with nucleophiles. Known iridium-isocyanide complexes [Ir(F$_2$ppy)$_2$(CNAr)$_2$]PF$_6$ (Ar = 4-trifluoromethylphenyl, 3,5-bis(trifluoromethyl)phenyl, and 4-nitrophenyl) with more electron-deficient aryl isocyanides have Δν values of 40–70 cm^{-1}.[3] ^{1}H and ^{13}C{^{1}H} NMR spectra of [**3a**–**d**](OTf) show a single sets of resonances for the ppy and isocyanide ligands suggesting C2 symmetry. Assignment of ^{1}H and ^{13}C{^{1}H} NMR signals was aided by ^{1}H,^{1}H-COSY, ^{1}H,^{13}C-HMQC/HSQC, and ^{1}H,^{13}C-HMBC NMR experiments.

1.2. Characterization of complexes [5a–d](OTf)

Diaminocarbene species [**5a**–**d**](OTf) were obtained as pale yellow solids in 73–86% yields; all [**5a**–**d**](OTf) are air- and moisture-stable at 20–160 °C. Complexes [**5a**–**d**](OTf) were characterized by elemental analyses (C, H, N), molar conductivity measurements, TG/DTA, high resolution ESI$^+$-MS, IR, 1D (^{1}H, ^{13}C{^{1}H}, ^{19}F{^{1}H}) and 2D (^{1}H,^{1}H-COSY, ^{1}H,^{13}C-HMQC/^{1}H,^{13}C-HSQC, ^{1}H,^{13}C-HMBC, ^{1}H,^{15}N-HSQC, and ^{1}H,^{15}N-HMBC) NMR spectroscopy. In addition, the structure of [**5b**](OTf) was elucidated by single-crystal X-ray diffraction. Complexes [**5a**–**d**](OTf) gave satisfactory CHN microanalyses, that are consistent with the proposed formulae. Values of molar conductivity for [**5a**–**d**](OTf) in acetonitrile (129–139 Ohm^{-1}cm^{-1}mol^{-1}) agree well with those for typical 1:1 electrolytes (120–160 Ohm^{-1}cm^{-1}mol^{-1} in MeCN[1]). HRESI$^+$-MS of [**5a**–

d](OTf) exhibit sets of peaks with the characteristic isotopic distribution due to $[M - OTf]^+$ ions. IR spectra of [**5a**–**d**](OTf) display no ν(C≡N) bands in the range between 2300 and 2100 cm^{-1}, supporting the transformation of the isocyanide ligands into the aminocarbenes. The medium-intensity bands 3201–3465 cm^{-1} in the IR spectra of [**5a**–**d**](OTf) are characteristic of ν(N–H) vibrations from the carbene moiety. In the ^1H NMR spectra the *bis*carbene complexes [**5a**–**d**](OTf), emergence of three broad signals, viz. δ_H 6.95, 7.27, and 7.78 ppm (ratio 1:1:1) due to NH protons suggests a restricted rotation of the NH_2 group around the C–N bond. $^{13}C\{^1H\}$ NMR are also consistent with the expected structure of [**5a**–**d**](OTf). Herein, addition of NH_3 to the isocyanide group is accompanied with a pronounced downfield δ ^{13}C shift of the isocyanide quaternary C atoms to the range that is specific for $M–C_{carbene}$ (δ_C 160–224 ppm).[4] The $C_{carbene}$ atoms in [**5a**–**d**](OTf) resonate at ca. δ_C 194 ppm that is ca. 60 ppm downfield-shifted *vs*. corresponded peaks in [**3a–d**](OTf) (*e.g.* δ_C 134.06 for C≡N in [**3b**](OTf)). Although no $^{13}C\{^1H\}$ NMR data for iridium(III)-ADC complexes have been reported, δ ^{13}C values for the $C_{carbene}$ atom in our [**5a**–**d**](OTf) are comparable to those in the known cyclometallated $(ADC)Pt^{II}$ complexes $[(CNN)Pt\{C(NHR^1)\text{-}(NHR^2)\}](ClO_4)$ (HCNN = 6-phenyl-2,2′-bipyridine; R^1 = *t*-Bu, Xyl, R^2 = Me, NH_2, CH_2Ph) (δ_C 185–194).[5]

1.3. Characterization of complexes [4a–d](OTf) and 6a–d

Complexes [**4b–d**](OTf) and **6a**–**d** were characterized by elemental analyses (C, H, N), molar conductivities (for [**4b–d**](OTf)), TG/DTA, high resolution ESI^+-MS, IR, 1D (^1H, $^{13}C\{^1H\}$, $^{19}F\{^1H\}$) and 2D (^1H,^1H-COSY, ^1H,^{13}C-HMQC/^1H,^{13}C-HSQC, ^1H,^{13}C-HMBC, ^1H,^{15}N-HSQC, and ^1H,^{15}N-HMBC) NMR spectroscopies. Complexes [**4b**–**d**](OTf) and **6a**–**d** gave satisfactory CHN microanalyses, that are consistent with the proposed formulae. The values of molar conductivities of [**4b**–**d**](OTf) in acetonitrile (135–145 $Ohm^{-1}cm^{-1}mol^{-1}$) agree with the typical range for 1:1 electrolytes (120–160 $Ohm^{-1}cm^{-1}mol^{-1}$ in MeCN[1]). The $HRESI^+$-MS of [**4b**–**d**](OTf), exhibit sets of peaks $[M - OTf]^+$ with the characteristic isotopic distribution. The $HRESI^+$-MS of **6a**–**d** exhibit quasi-molecular ion peaks ($[M + H]^+$ and $[M + Na]^+$) and set of peaks from $[M - CN]^+$. In the IR spectra of mixed isocyanide–diaminocarbene complexes [**4b**–**d**](OTf), we observed only one CN stretching vibration at 2139–2145 cm^{-1} from isocyanide ligand. The IR spectra of **6a**–**d** display one strong ν(C≡N) band in the interval 2090–2092 cm^{-1}, which emerge at almost the same frequencies as the *C*-coordinated cyanide group in the iridium(III) complex $[n\text{-}Bu_4N][Ir(ppy)_2(CN)_2]$ (ν(C≡N) 2092 cm^{-1}).[6] The N–H resonances in the ^1H NMR spectra of [**4b**–**d**](OTf) and **6a**–**d** were not detected. The $C_{carbene}$=NH atoms in [**4b**–**d**](OTf) and **6a**–**c** were found to resonate at ca. δ_C 189 ppm and ca. δ_C 193 ppm, respectively; insufficient solubility of **6d** precluded ^{13}C measurements.

Table S1. C≡N stretching vibration frequency of uncomplexed isocyanides **2a–d** and complexes [**3a–d**](OTf)

X	**ν (C≡N), см$^{-1}$**		
	2	[**3**](OTf)	Δν
a: X = F	2129	2156; 2184	+27
b: X = Cl	2123	2151; 2179	+28
c: X = Br	2123	2151; 2180	+28
d: X = I	2140	2145; 2173	+5

Table S2. ^{1}H NMR monitoring of reaction[a] between [**3c**](OTf) and NH_3

No.	**Time**	**[3c](OTf)**	**[4c](OTf)**	**[5c](OTf)**	**6c**
1	0	100%	0%	0%	0%
2	1 h	80%	20%	0%	0%
3	2 h	45%	55%	0%	0%
4	3 h	20%	70%	10%	0%
5	10 h	0%	50%	50%	0%
6	1 d	0%	30%	60%	10%
7	4 d	0%	10%	30%	60%
8	6 d	0%	0%	15%	85%
9	8 d	0%	0%	0%	100%

[a]Reaction conditions: complex [**3c**](OTf) (0.005 mmol) was suspended in CD_2Cl_2 (1 mL) in a small glass vial. Vial was carefully placed in a larger scintillation flask (20mL) containing 5mL of aqueous ammonia (14M) at the bottom and kept at RT for the duration of reaction.

Table S3. Overall ^{1}H NMR yield and a ratio between [**4c**](OTf) and **6c** in the reaction between [**5c**](OTf) and bases.

Solvent and reagents	Time	Overall ^{1}H NMR yield of [4c](OTf) and 6c, %	Ratio between [4c](OTf) and 6c
CH_2Cl_2, gaseous NH_3 atmosphere ($pK_a = 9.25$)[a], RT	8 d	>99	only **6c**
$C_2H_4Cl_2$, gaseous NH_3 atmosphere ($pK_a = 9.25$)[a], 50 °C	3 d	>99	only **6c**
MeOH, gaseous NH_3 atmosphere ($pK_a = 9.25$)[a], 50 °C	12 h	52	only **6c**
MeOH, gaseous NH_3 atmosphere ($pK_a = 9.25$)[a], 50 °C	1 d	72	only **6c**
MeOH, gaseous NH_3 atmosphere ($pK_a = 9.25$)[a], 50 °C	2 d	96	only **6c**
MeOH, gaseous NH_3 atmosphere ($pK_a = 9.25$)[a], 50 °C	3 d	>99	only **6c**
MeOH, $(HOCH_2CH_2)_3N$ ($pK_a = 7.74$)[a,b], 50 °C	2 d	>99	only **[4c](OTf)**
MeOH, pyridine ($pK_a = 5.25$)[a,b], 50 °C	2 d	>99	only **[4c](OTf)**
MeOH, *N*-methylmorpholine ($pK_a = 7.38$)[a,b], 50 °C	2 d	>99	only **[4c](OTf)**
MeOH, NH_4Cl (excess)+ K_2CO_3[c], 50 °C	2 d	>99	only **[4c](OTf)**
MeOH, NH_4Cl (excess)+ KOH[c], 50 °C	2 d	>99	only **[4c](OTf)**
MeOH, Et_3N ($pK_a = 10.75$)[a,b], 50 °C	12 h	41	1:1
MeOH, Et_3N ($pK_a = 10.75$)[a,b], 50 °C	1 d	60	1:1
MeOH, Et_3N ($pK_a = 10.75$)[a,b], 50 °C	2 d	>99	1:1
MeOH, KOH[b], 50 °C	1 d	>99	1:1
MeOH, NH_4Cl[b], 50 °C	1 d	0	–
MeOH, 50 °C	4 d	0	–

[a]The pKa of the conjugate acid in water. [b]Ratio [**5c**](OTf) to organic base was 1:2. [c]Ratio [**5c**](OTf):NH_4Cl:base is 1:10:1.

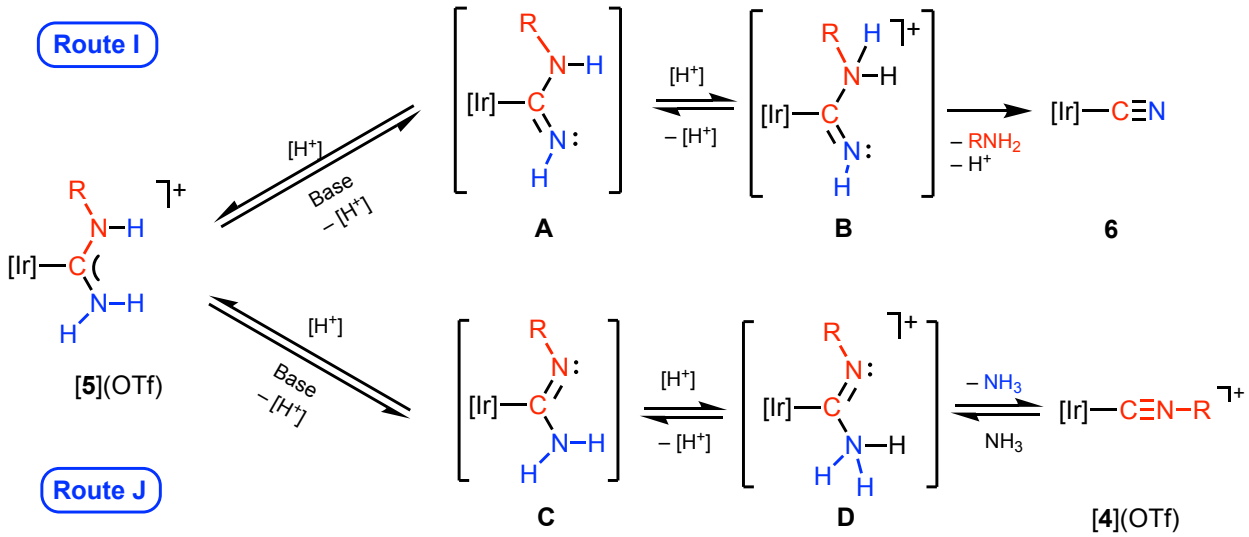

Scheme S1. Proposed mechanism of base-mediated cleavage of ADC ligands in [**5a–d**](OTf).

Table S4. Crystal data and structures refinement.

Identification code	*[**3b**](OTf)*	*[**3c**](OTf)*
Empirical formula	$C_{37}H_{24}Cl_2F_3IrN_4O_3S$	$C_{37}H_{24}Br_2F_3IrN_4O_3S$
Formula weight	924.76	1013.68
Temperature/K	100(2)	100(2)
Crystal system	monoclinic	monoclinic
Space group	$P2_1/n$	$P2_1/c$
a/Å	11.1328(3)	10.89737(11)
b/Å	14.0956(4)	21.25955(19)
c/Å	22.0626(7)	15.54005(14)
α/°	90	90
β/°	100.734(2)	95.7060(8)
γ/°	90	90
Volume/Å^3	3401.55(17)	3582.37(6)
Z	4	4
ρ_{calc}g/cm^3	1.806	1.879
μ/mm^{-1}	4.205	10.877
F(000)	1808.0	1952.0
Crystal size/mm^3	0.2 × 0.2 × 0.15	0.15 × 0.15 × 0.08
Radiation	MoKα (λ = 0.71073)	CuKα (λ = 1.54184)
2Θ range for data collection/°	5.326 to 54.998	7.068 to 152.89
Index ranges	$-14 \le h \le 8$, $-18 \le k \le 11$, $-23 \le l \le 28$	$-13 \le h \le 13$, $-26 \le k \le 26$, $-19 \le l \le 19$
Reflections collected	15753	44094
Independent reflections	7606 [R_{int} = 0.0272, R_{sigma} = 0.0425]	7487 [R_{int} = 0.0475, R_{sigma} = 0.0260]
Data/restraints/parameters	7606/0/460	7487/0/460
Goodness-of-fit on F^2	1.181	1.034
Final R indexes [I>=2σ (I)]	R_1 = 0.0347, wR_2 = 0.0689	R_1 = 0.0300, wR_2 = 0.0779
Final R indexes [all data]	R_1 = 0.0451, wR_2 = 0.0732	R_1 = 0.0313, wR_2 = 0.0793
Largest diff. peak/hole / e Å^{-3}	1.52/-0.83	1.77/-1.05
CCDC numbers	1538183	1538181

Identification code	*[**4b**](OTf)*	*[**5b**](OTf)*	***6c***
Empirical formula	$C_{36}H_{26}Cl_2IrN_5$	$C_{38}H_{31}Cl_5F_3IrN_6O_3S$	$C_{31}H_{24}BrCl_3IrN_5$
Formula weight	791.72	1078.20	845.01
Temperature/K	100(2)	100(2)	100(2)
Crystal system	monoclinic	monoclinic	monoclinic
Space group	$P2_1/c$	$P2_1/c$	$P2_1/c$
a/Å	11.3436(7)	13.0467(8)	14.0167(3)
b/Å	22.3709(10)	30.1504(13)	12.4881(2)
c/Å	13.9967(8)	10.5444(5)	19.1229(3)
α/°	90	90	90
β/°	94.676(6)	100.392(6)	105.7660(19)
γ/°	90	90	90
Volume/Å^3	3540.1(3)	4079.7(4)	3221.38(10)
Z	4	4	4
ρ_{calc}g/cm^3	1.485	1.755	1.742
μ/mm^{-1}	3.953	3.711	11.993
F(000)	1552.0	2120.0	1632.0
Crystal size/mm^3	0.2 × 0.2 × 0.2	0.1 × 0.1 × 0.08	0.15 × 0.15 × 0.1
Radiation	MoKα (λ = 0.71073)	MoKα (λ = 0.71073)	CuKα (λ = 1.54184)
2Θ range for data collection/°	5.75 to 55	5.404 to 55	6.552 to 152.658
Index ranges	$-14 \le h \le 14$, $-29 \le k \le 28$, $-18 \le l \le 18$	$-15 \le h \le 16$, $-39 \le k \le 32$, $-13 \le l \le 10$	$-17 \le h \le 17$, $-14 \le k \le 15$, $-24 \le l \le 16$
Reflections collected	23108	20065	27500
Independent reflections	8132 [R_{int} = 0.0307, R_{sigma} = 0.0371]	9356 [R_{int} = 0.0689, R_{sigma} = 0.1006]	6699 [R_{int} = 0.0890, R_{sigma} = 0.0507]
Data/restraints/parameters	8132/0/397	9356/0/481	6699/6/371
Goodness-of-fit on F^2	1.184	1.252	1.030
Final R indexes [I>=2σ (I)]	R_1 = 0.0554, wR_2 = 0.1096	R_1 = 0.0765, wR_2 = 0.1371	R_1 = 0.0514, wR_2 = 0.1331
Final R indexes [all data]	R_1 = 0.0689, wR_2 = 0.1159	R_1 = 0.0896, wR_2 = 0.1425	R_1 = 0.0601, wR_2 = 0.1427
Largest diff. peak/hole / e Å^{-3}	2.95/-2.36	2.10/-3.15	2.40/-3.07
CCDC numbers	1538186	1538184	1538185

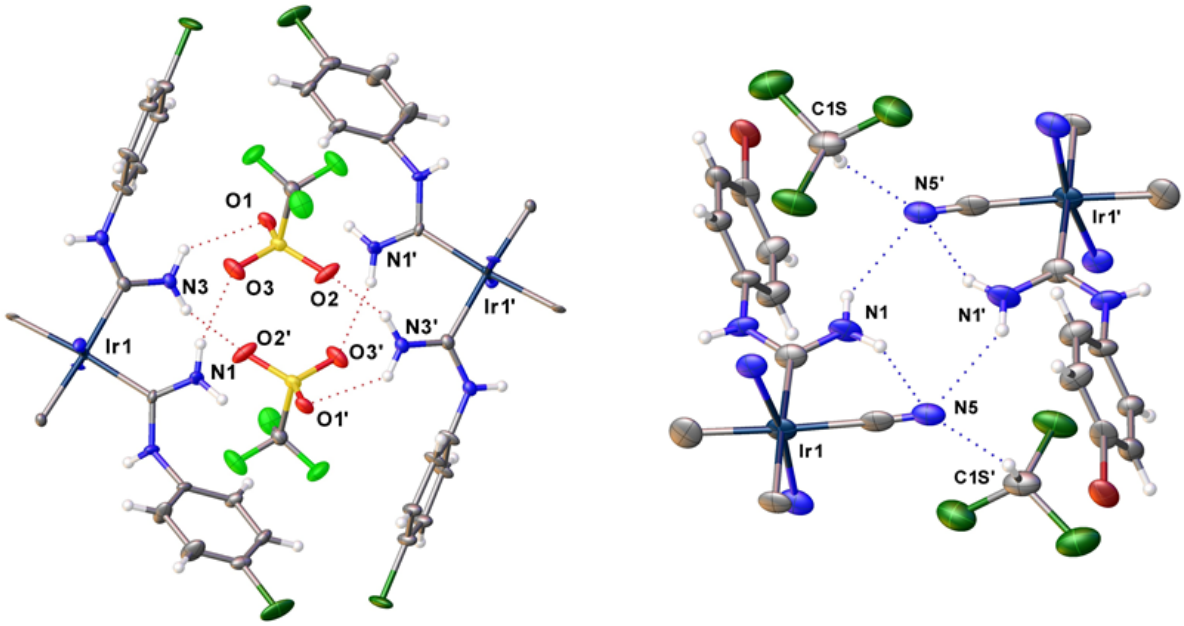

Figure S1. View of the H-bonded dimeric associates of [**5b**](OTf) (left) and **6c** (right) with the intermolecular and intramolecular hydrogen bonds. Cyclometalated ligand fragments were omitted for simplicity.

Table S5. Selected H-bond lengths and angles for [**5b**](OTf) and **6c**

[**5b**](OTf)		**6c**	
Bond lengths, Å			
N1–H···O3	3.014(9)	N1–H···N5	3.115(9)
N1'–H···O3'	3.014(9)	N1–H···N5'	3.401(8)
N3–H···O1	2.994(8)	N5–H···C1S	3.225(6)
N3–H···O2'	2.883(11)	N1'–H···N5'	3.115(9)
N3'–H···O1'	2.994(8)	N1'–H···N5	3.401(8)
N3'–H···O2	2.883(11)	N5'–H···C1S'	3.225(6)
Bond angles, °			
N1–H···O3	161.36(8)	N1–H···N5	145.10(8)
N1'–H···O3'	161.36(8)	N1–H···N5'	135.61(7)
N3–H···O1	125.95(6)	N5–H···C1S	145.65(5)
N3–H···O2'	155.90(7)	N1'–H···N5'	145.10(8)
N3'–H···O1'	125.95(6)	N1'–H···N5	135.61(7)
N3'–H···O2	155.90(7)	N5'–H···C1S'	145.65(5)

In the crystal structure of [**5b**](OTf), N–H···O hydrogen bonds (HBs) between triflate anion from the first molecule and the carbene NH_2 protons of the other molecule, can be recognized. A system of six N–H···O intermolecular HBs link two organometallic cations and two

triflate anions into H-bonded dimeric associates. The heavy atom distance in N3–H···O2' (2.883(11) Å) contact between the NH_2 of the carbene groups and the triflate anion is approximately 0.19 Å shorter than the sum of the Bondi's van der Waals radii for the O and N atoms (3.07 Å[1]). At the same time longer distances in N3–H···O1 (2.994(8) Å) and N1–H···O3 (3.014(9) Å) contacts indicate that these H-bonds between the NH_2 of the carbene groups and the triflate anion are rather weak.

In the crystal structure of **6c**, intermolecular interactions lead to dimeric associates. Hence in this complex, each NH_2 group interacts with two cyanide groups from different molecules giving H-bonded dimers.

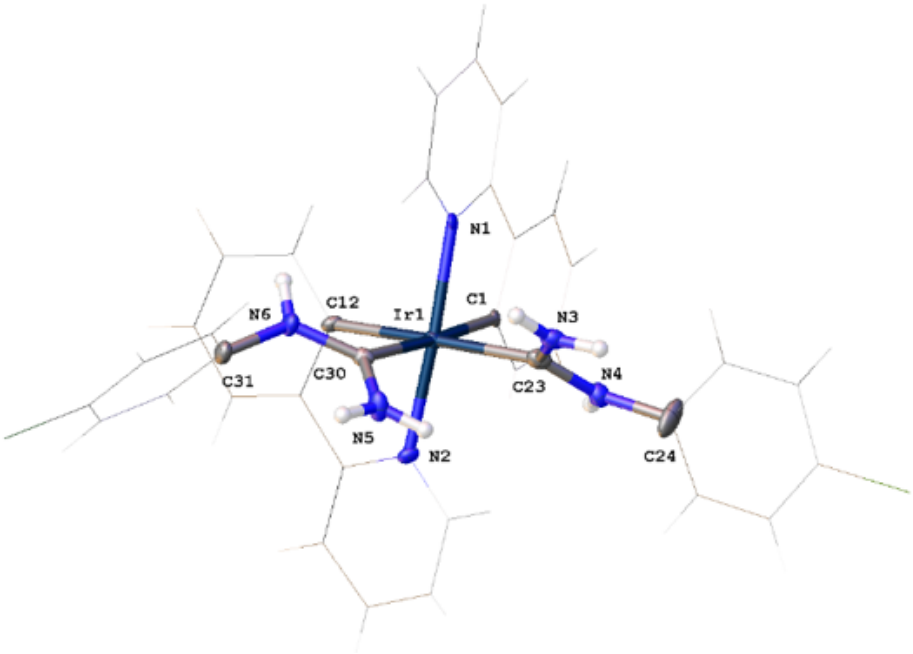

Figure S2. Mutual arrangement of the ADC moieties in [**5b**]$^+$.

NMR spectra

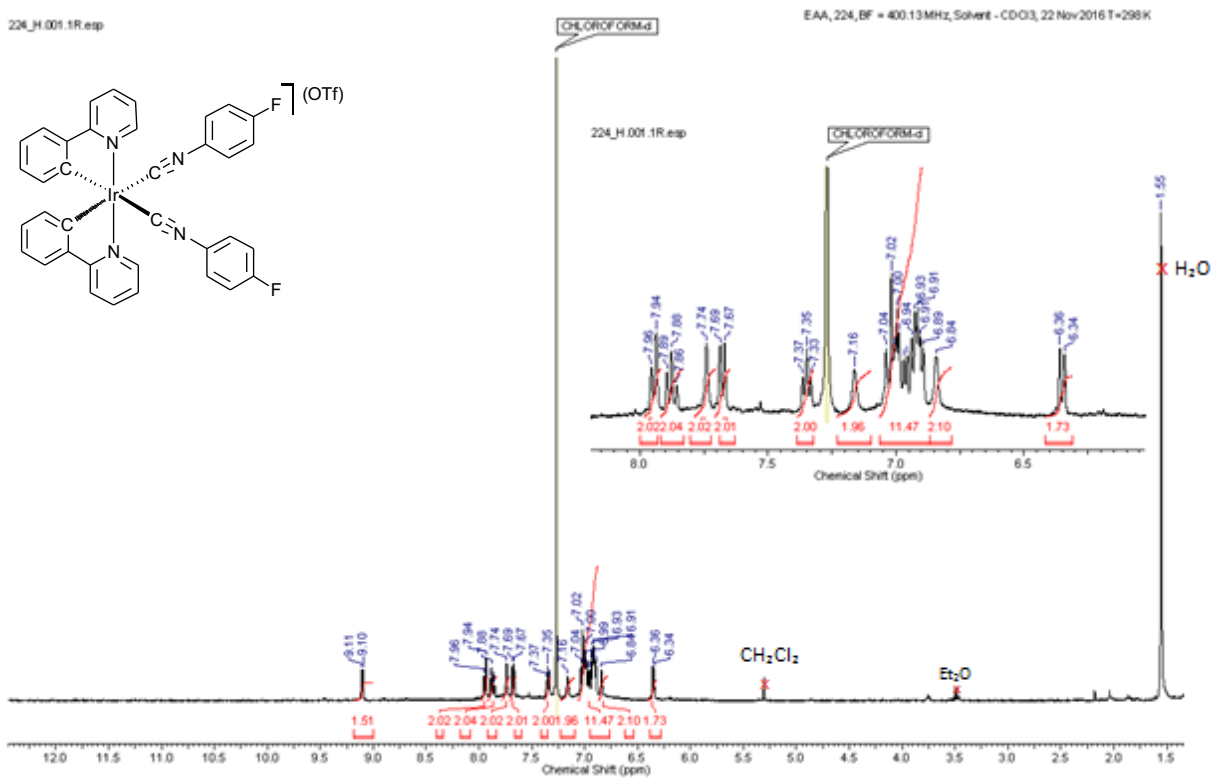

Figure S3. ^{1}H NMR spectrum of [**3a**](OTf) in $CDCl_3$

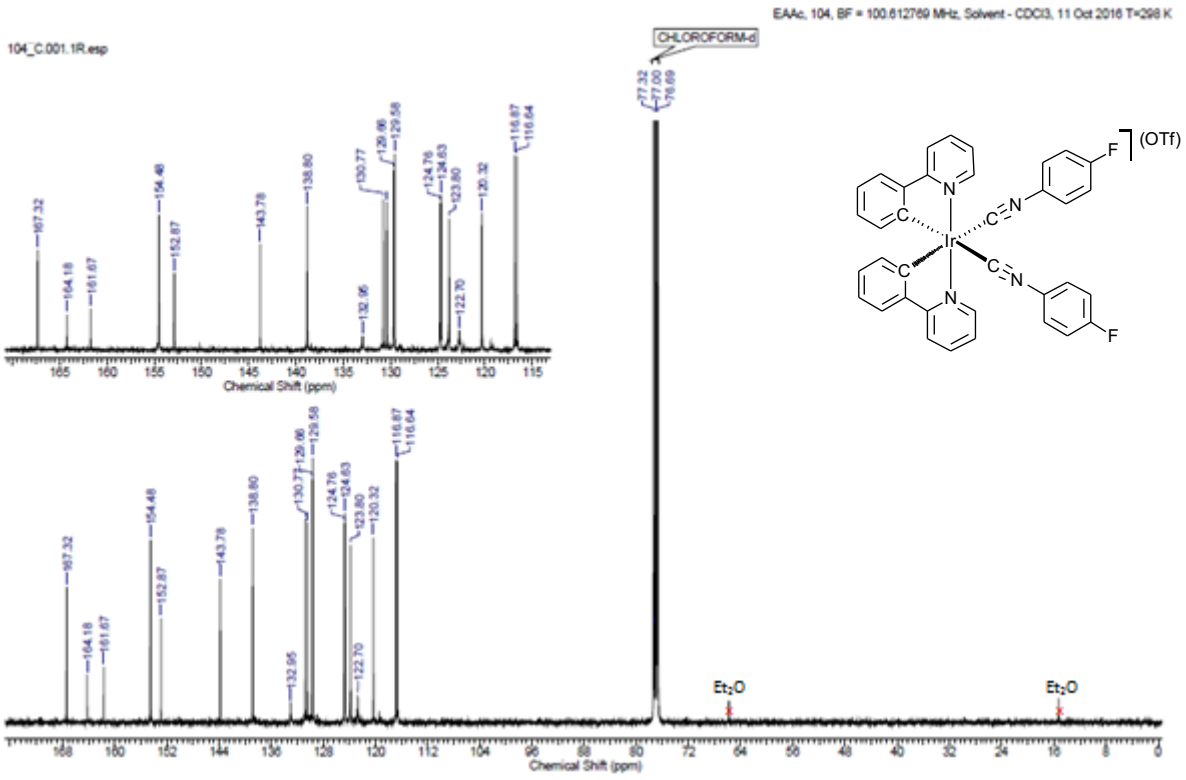

Figure S4. $^{13}C\{^{1}H\}$ NMR spectrum of [**3a**](OTf) in $CDCl_3$

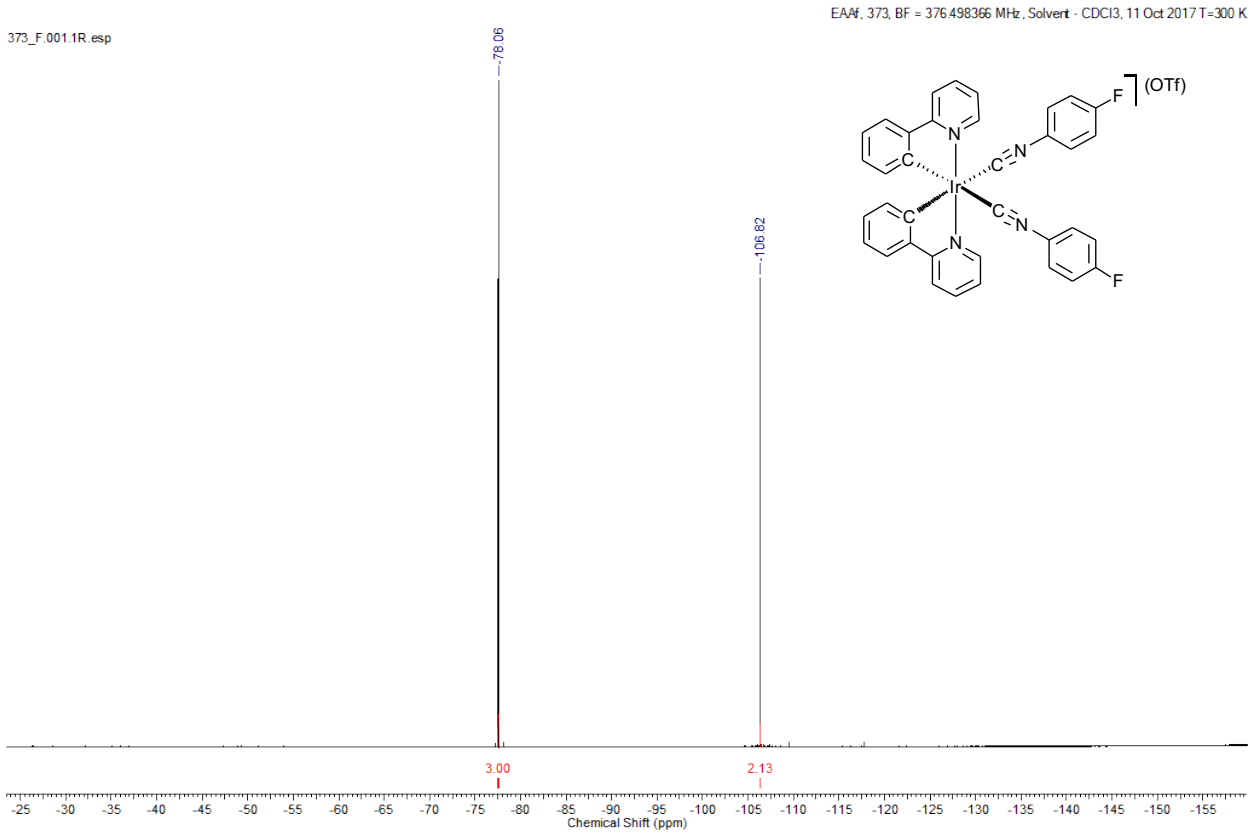

Figure S5. $^{19}F\{^{1}H\}$ NMR spectrum of [**3a**](OTf) in $CDCl_3$

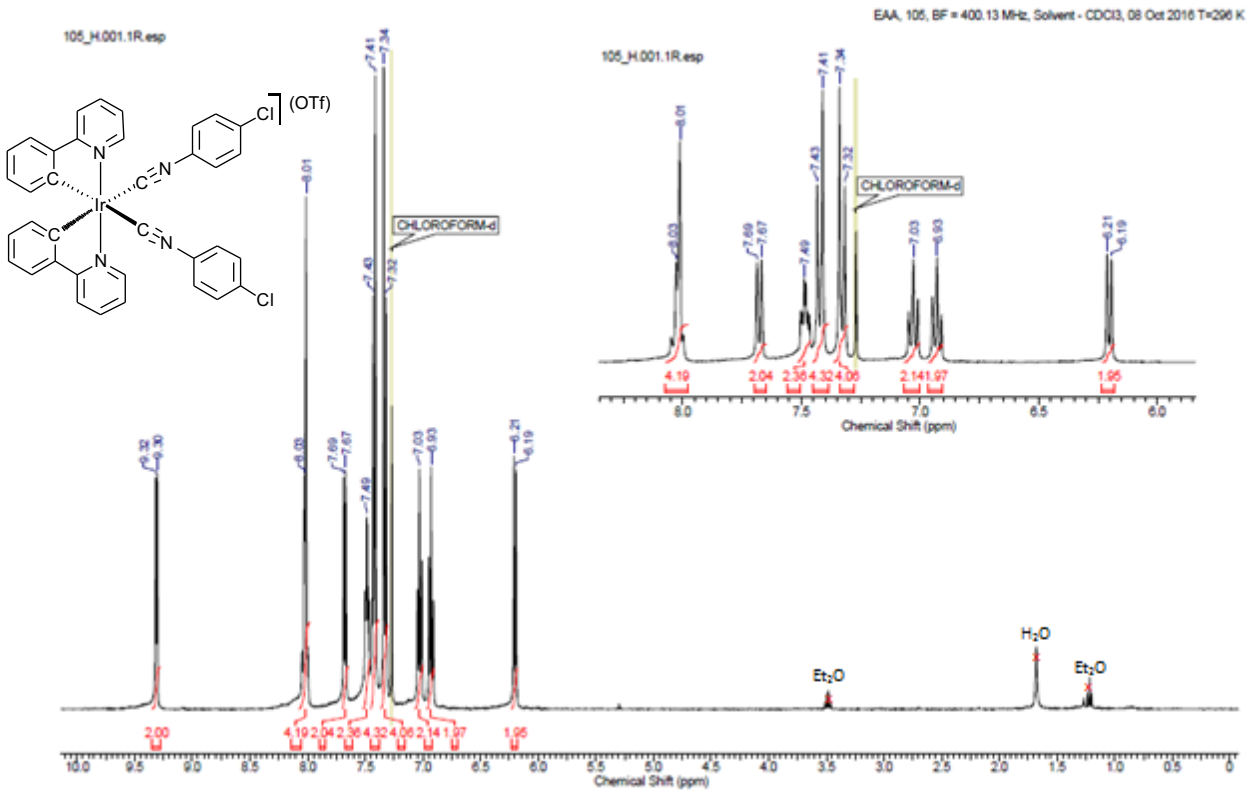

Figure S6. ^{1}H NMR spectrum of [**3b**](OTf) in $CDCl_3$

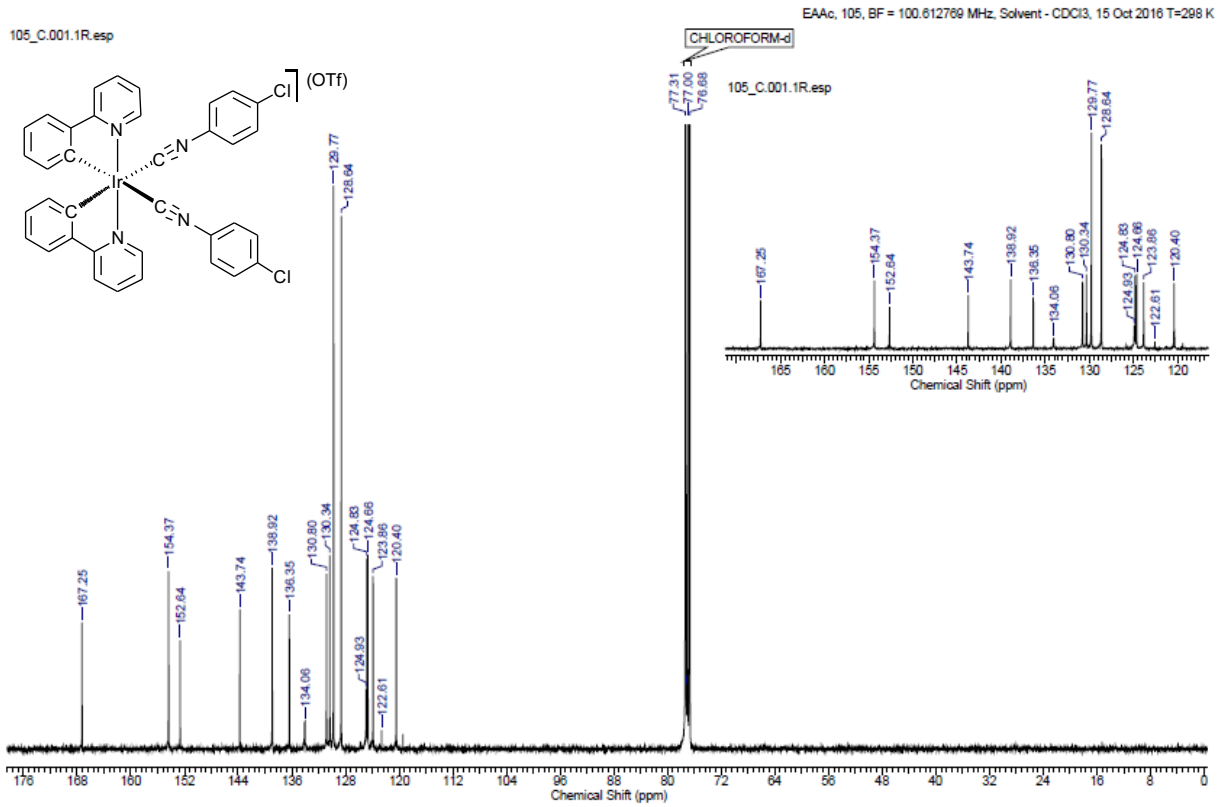

Figure S7. $^{13}C\{^{1}H\}$ NMR spectrum of [**3b**](OTf) in $CDCl_3$

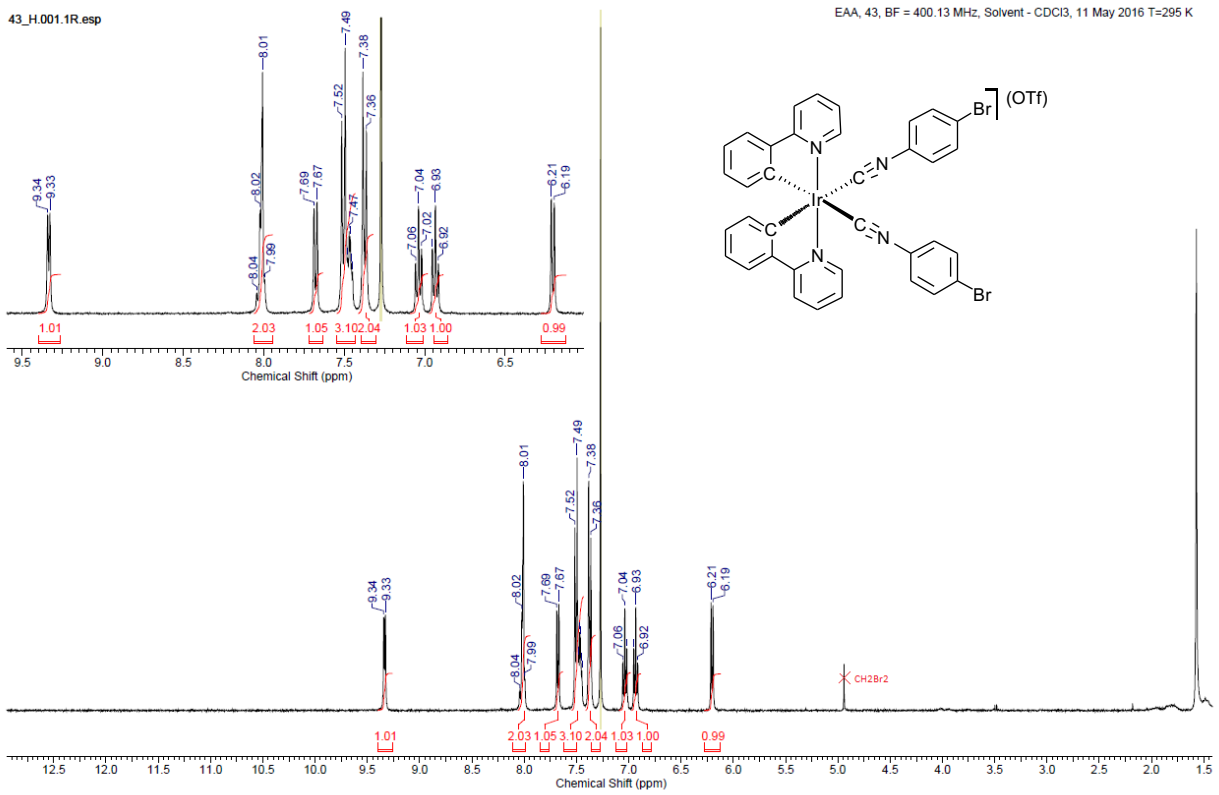

Figure S8. ^{1}H NMR spectrum of [**3c**](OTf) in $CDCl_3$

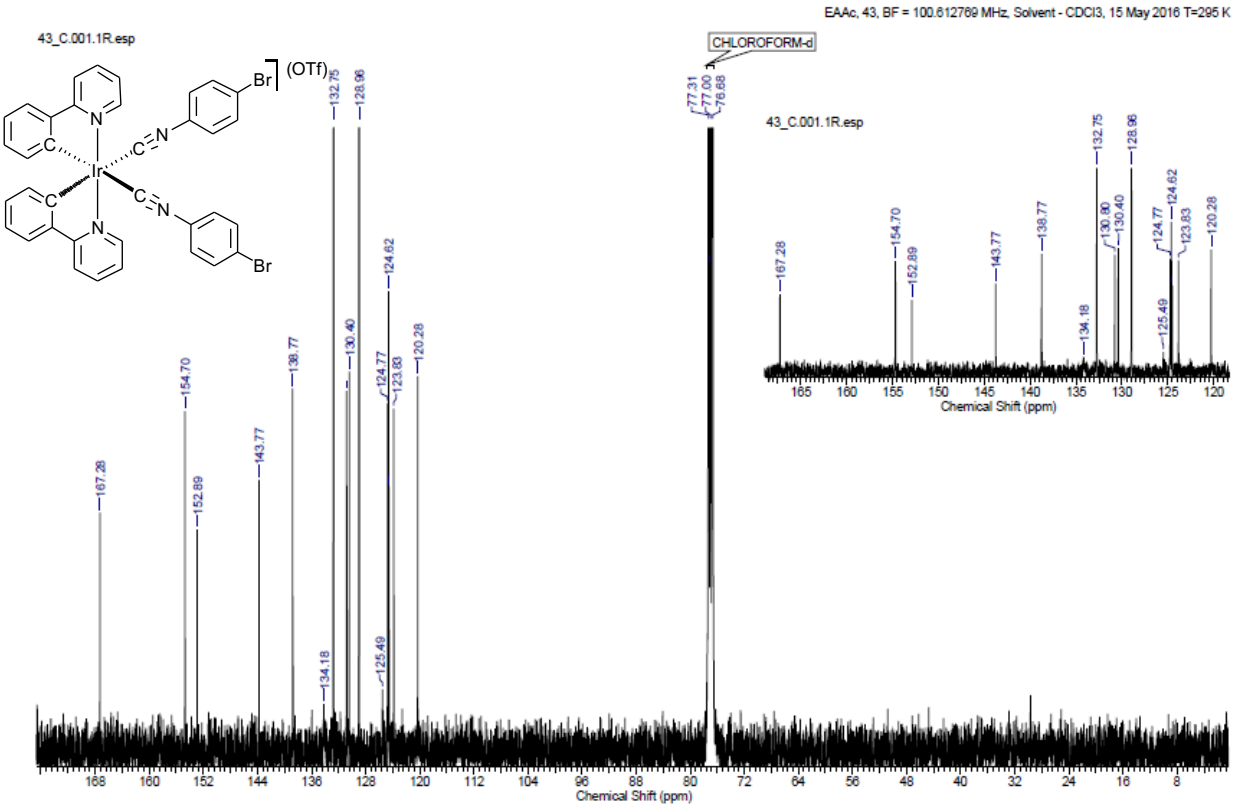

Figure S9. ^{13}C{^{1}H} NMR spectrum of [**3c**](OTf) in $CDCl_3$

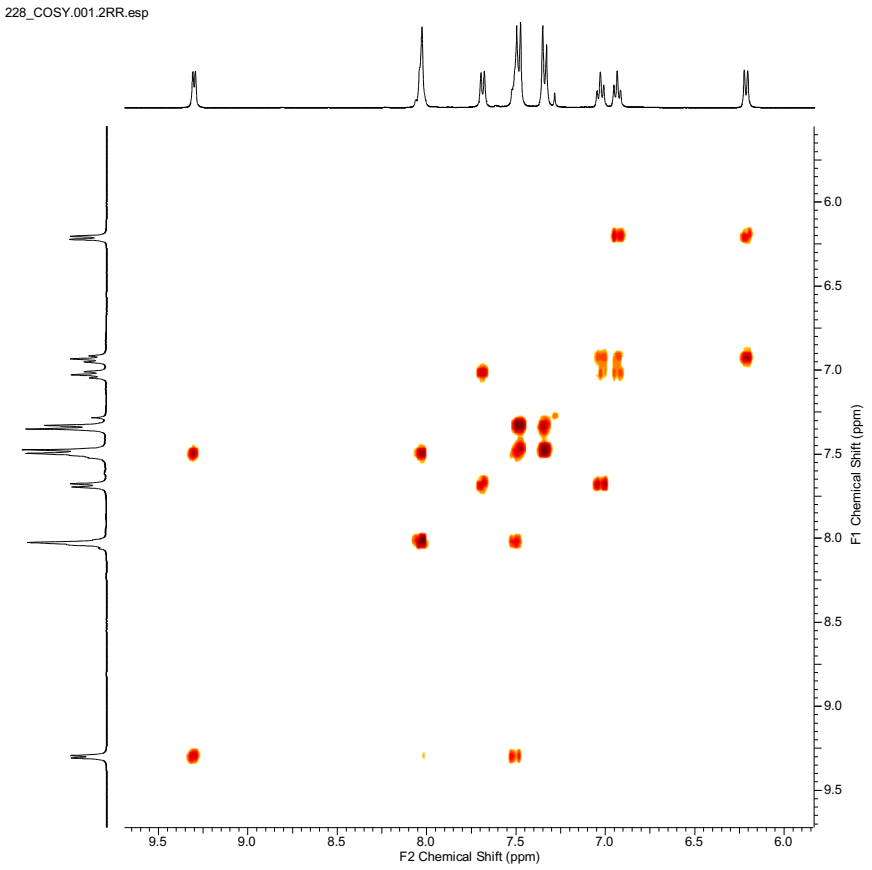

Figure S10. $^{1}H,^{1}H$-COSY NMR spectrum of [**3c**](OTf) in $CDCl_3$

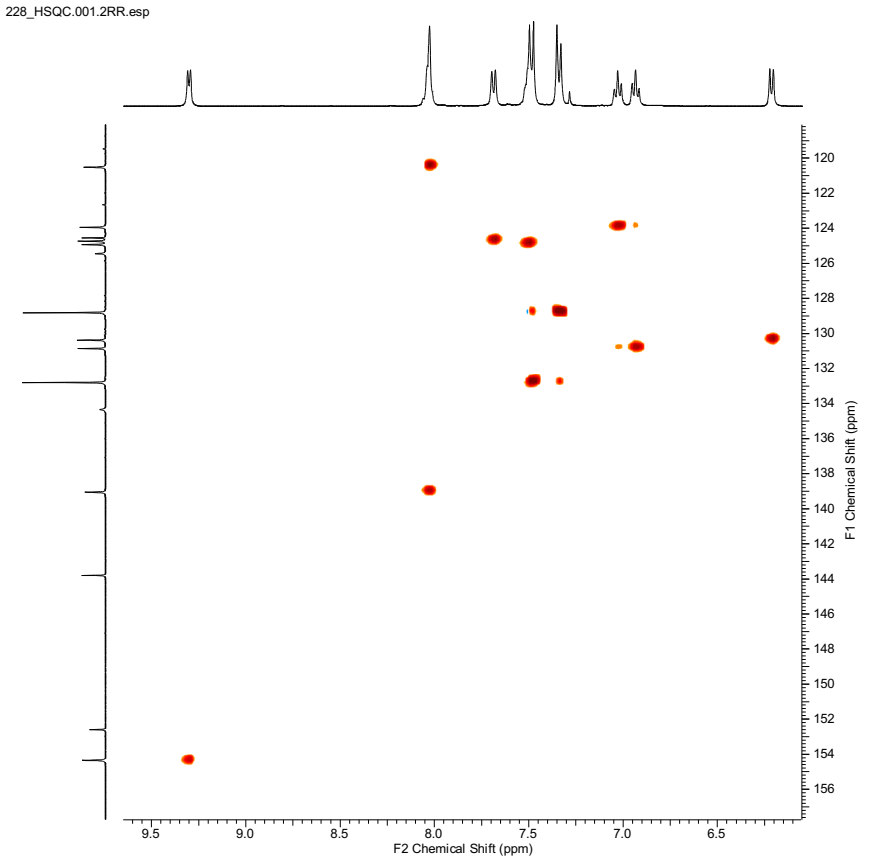

Figure S11. $^{1}H,^{13}C$-HSQC NMR spectrum of [**3c**](OTf) in $CDCl_3$

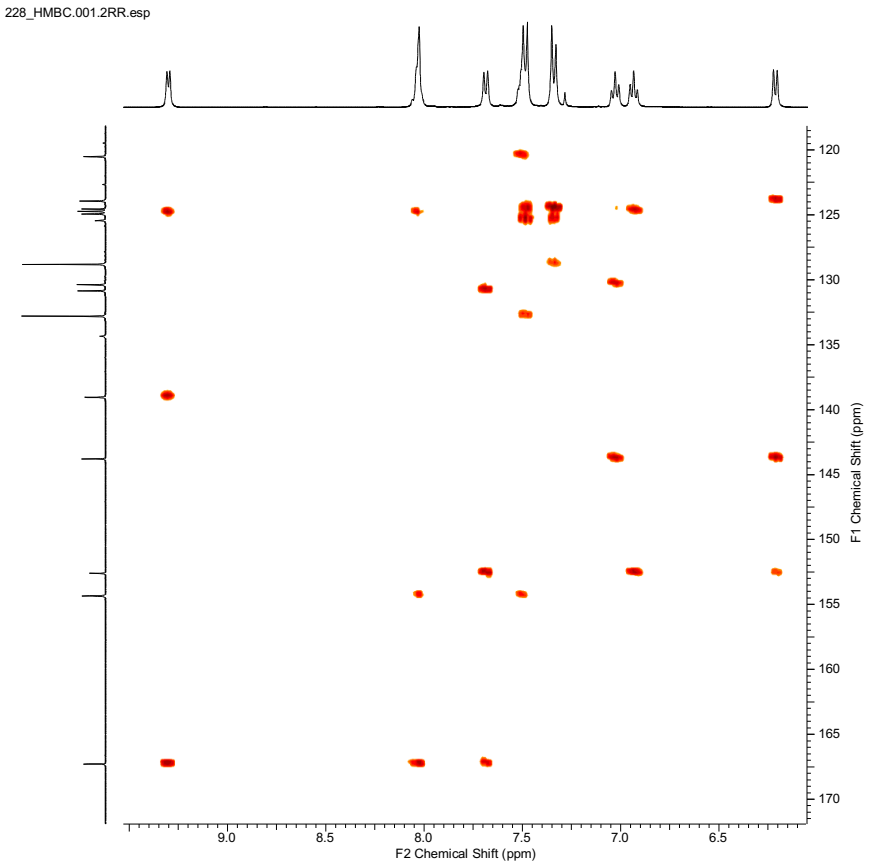

Figure S12. $^{1}H,^{13}C$-HMBC NMR spectrum of [**3c**](OTf) in $CDCl_3$

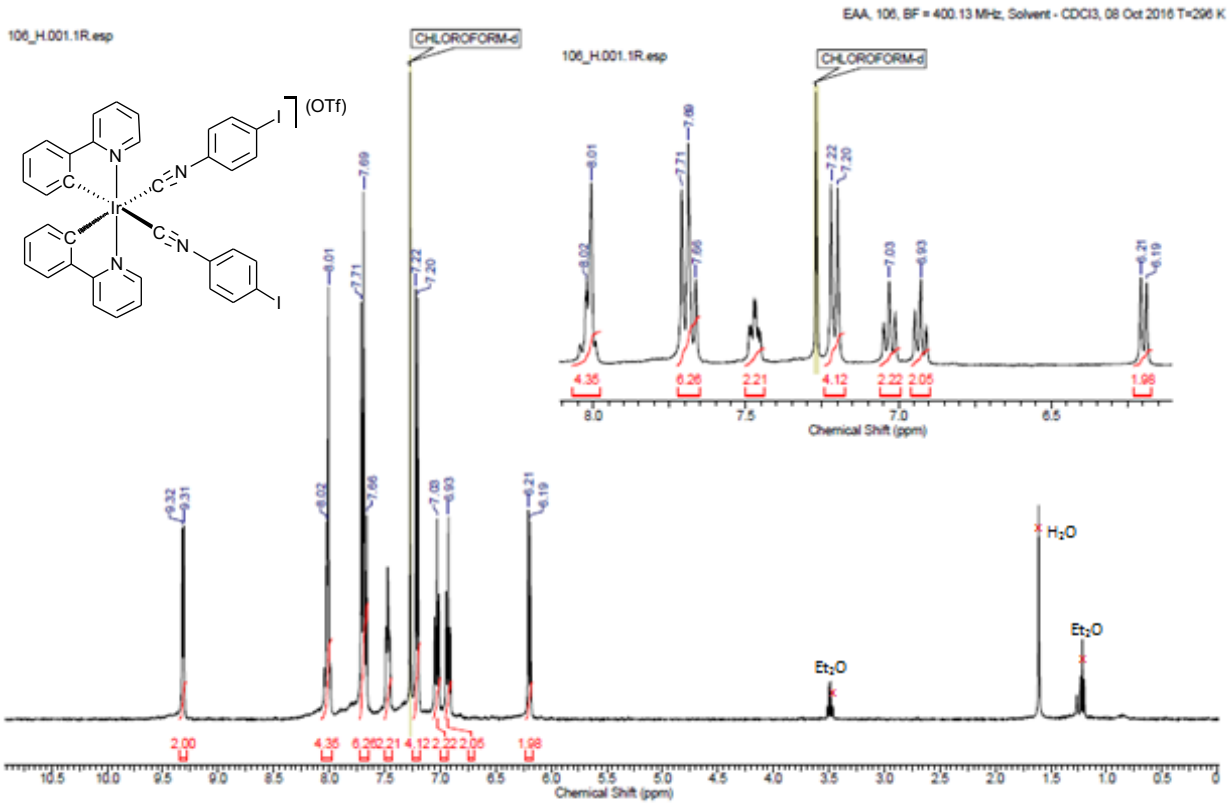

Figure S13. ^{1}H NMR spectrum of [**3d**](OTf) in $CDCl_3$

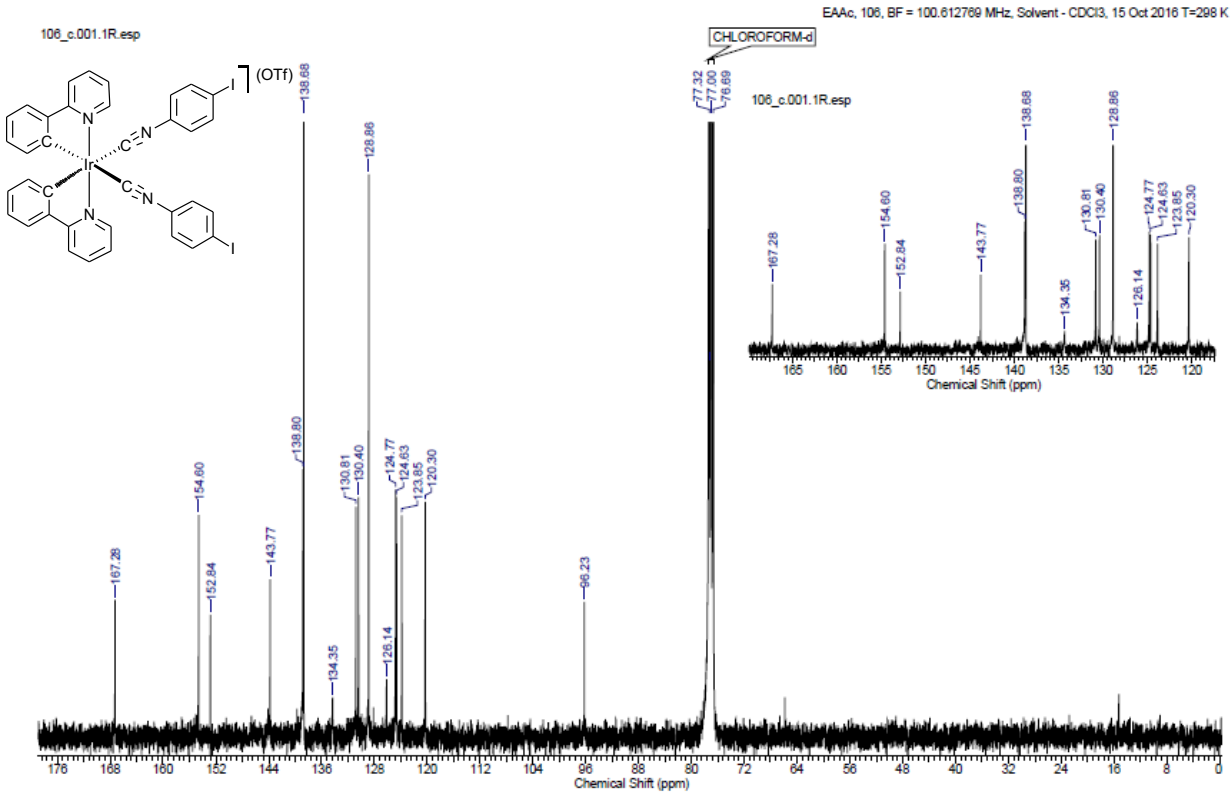

Figure S14. ^{13}C{^{1}H} NMR spectrum of [**3d**](OTf) in $CDCl_3$

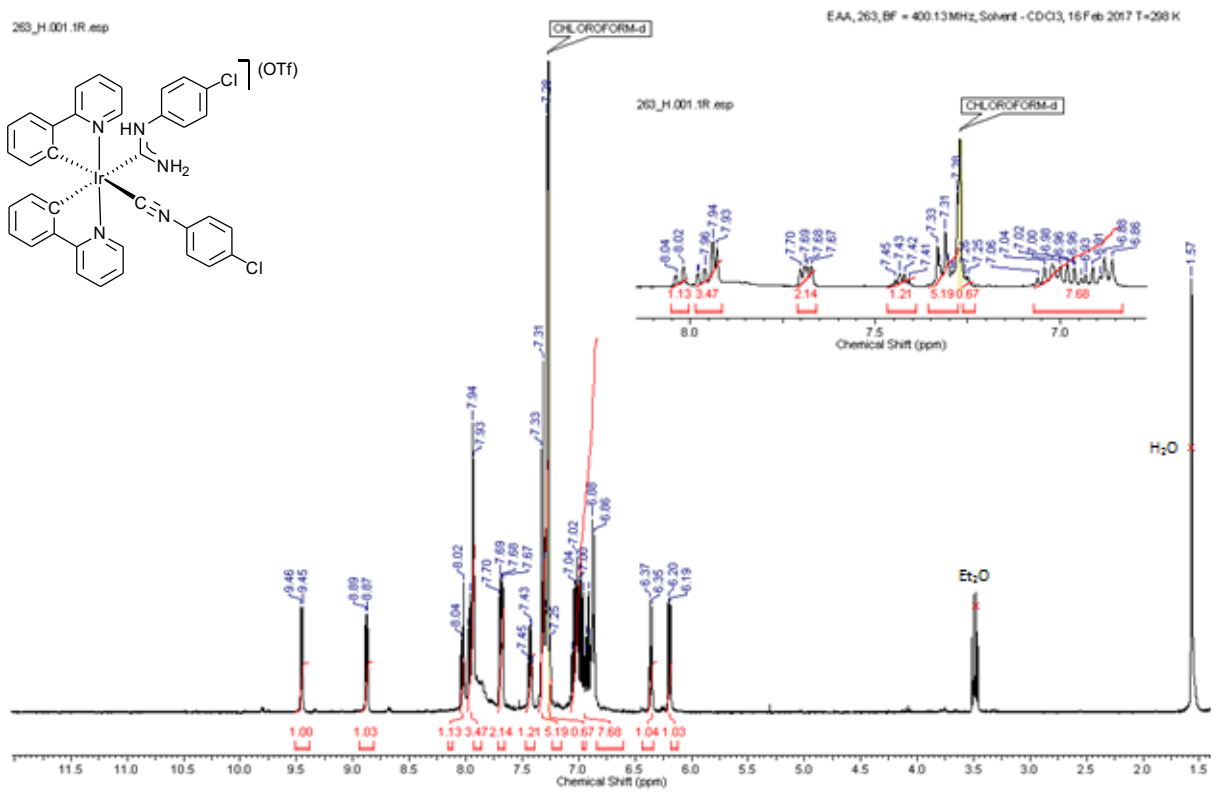

Figure S15. ^{1}H NMR spectrum of [**4b**](OTf) in $CDCl_3$

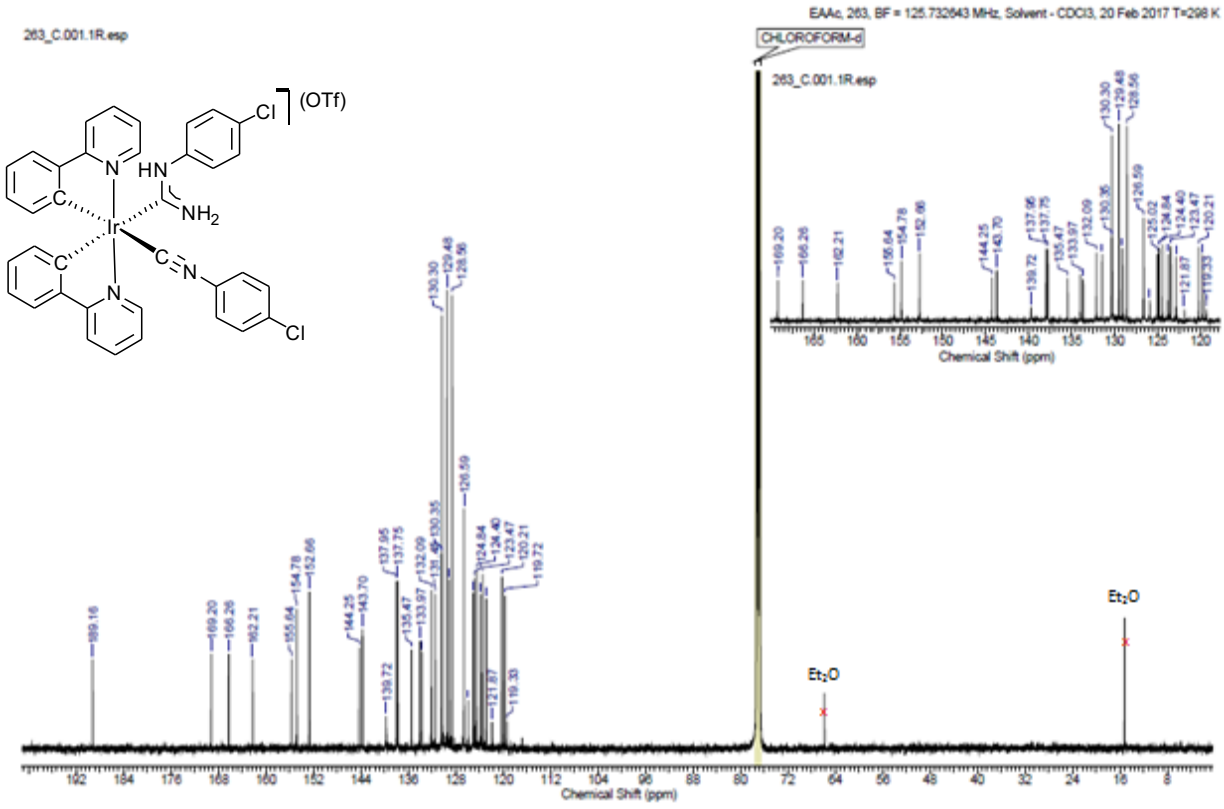

Figure S16. $^{13}C\{^{1}H\}$ NMR spectrum of [**4b**](OTf) in $CDCl_3$

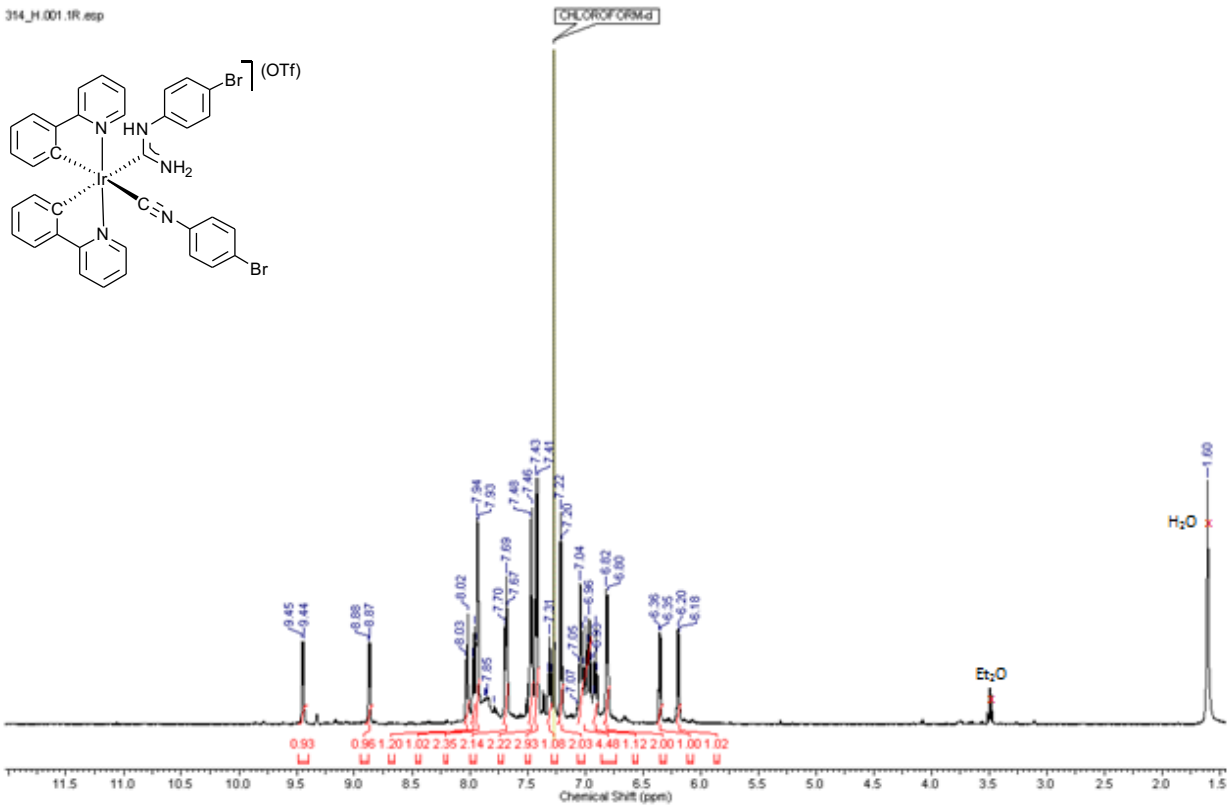

Figure S17. ^{1}H NMR spectrum of [**4c**](OTf) in $CDCl_3$

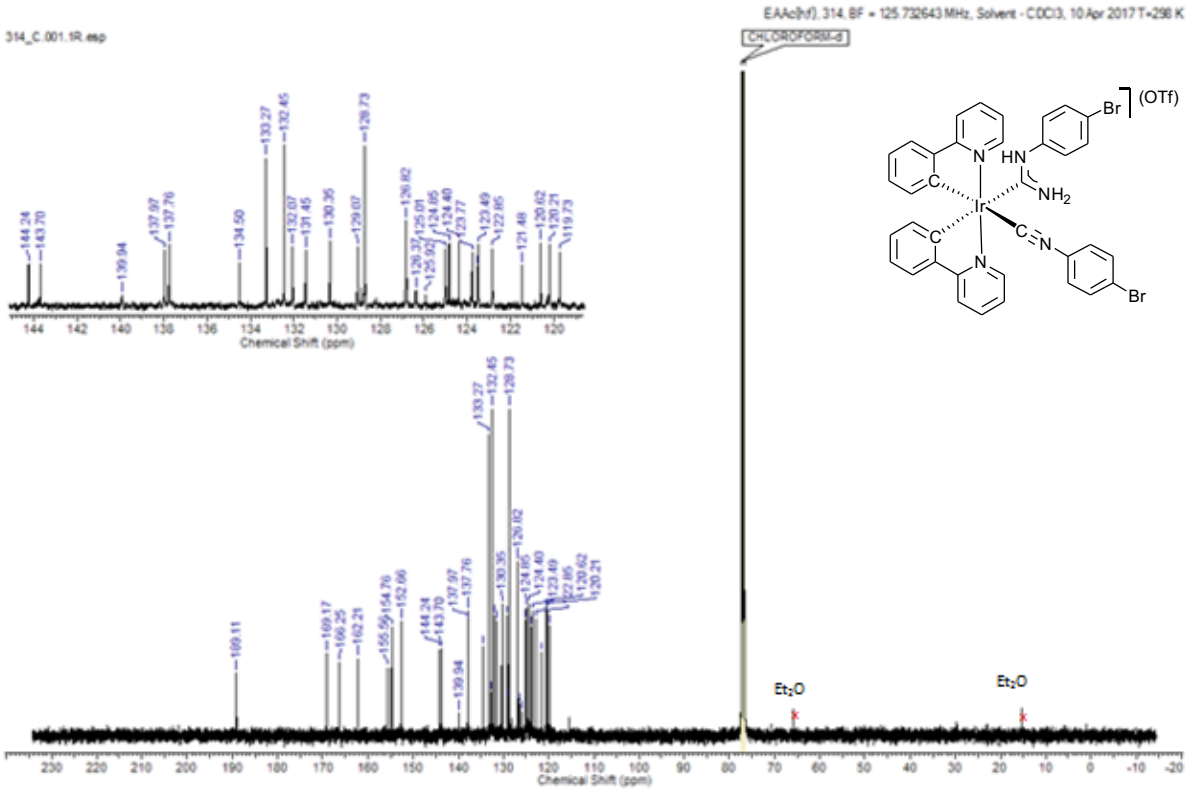

Figure S18. ^{13}C{^{1}H} NMR spectrum of [**4c**](OTf) in $CDCl_3$

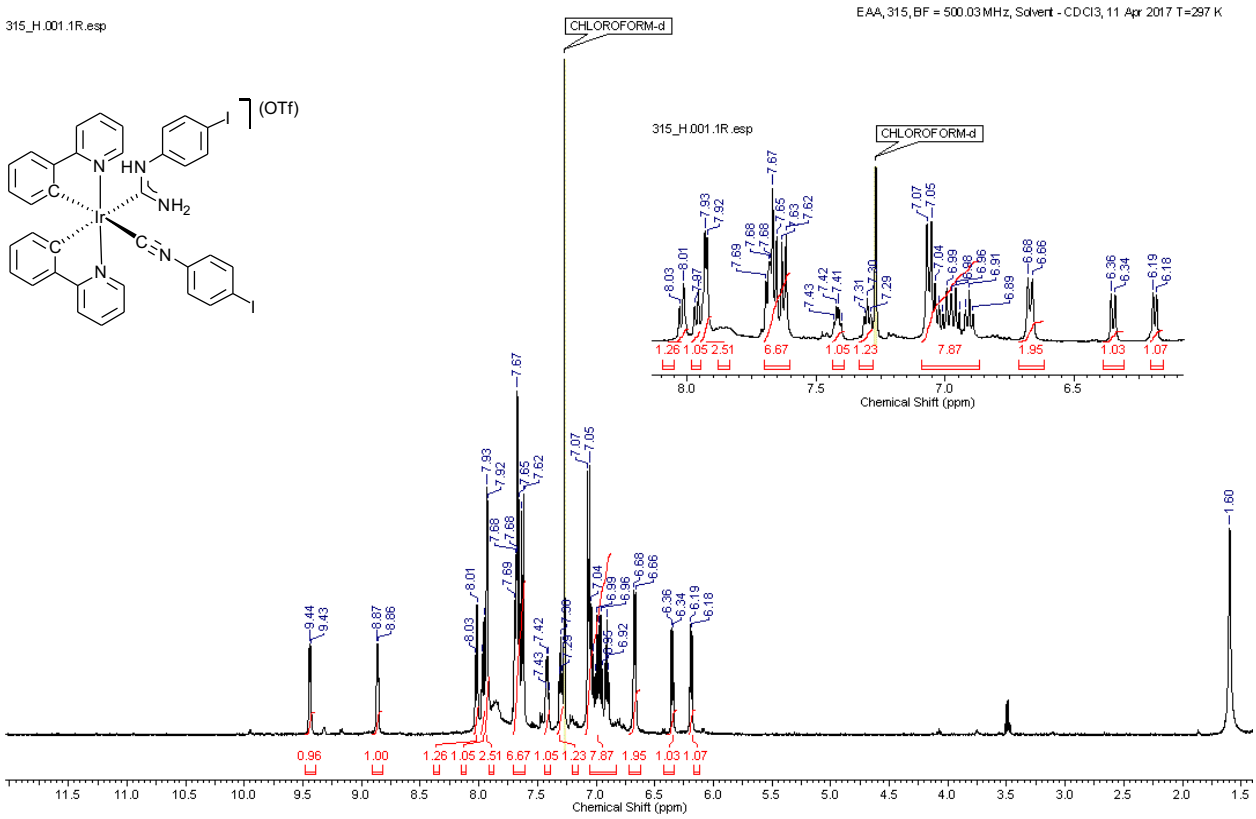

Figure S19. ^{1}H NMR spectrum of [**4d**](OTf) in $CDCl_3$

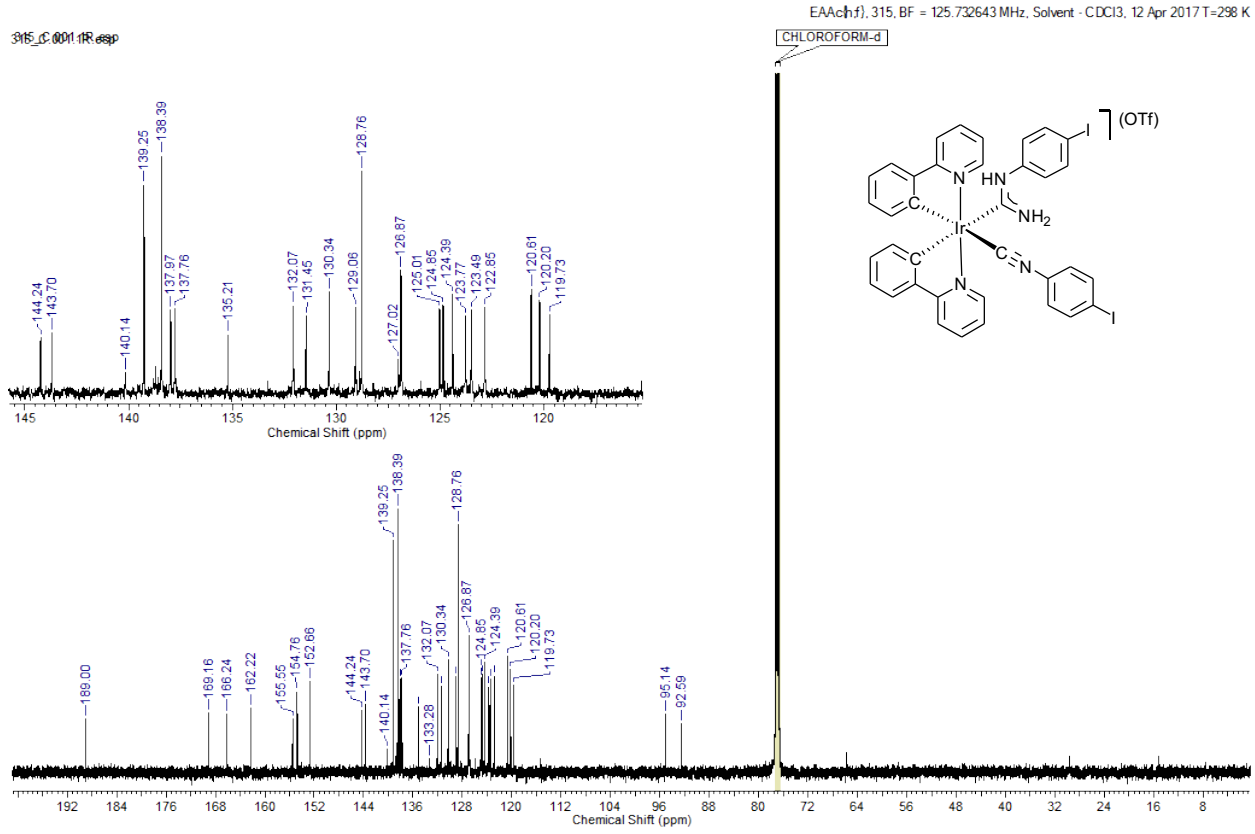

Figure S20. $^{13}C\{^{1}H\}$ NMR spectrum of [**4d**](OTf) in $CDCl_3$

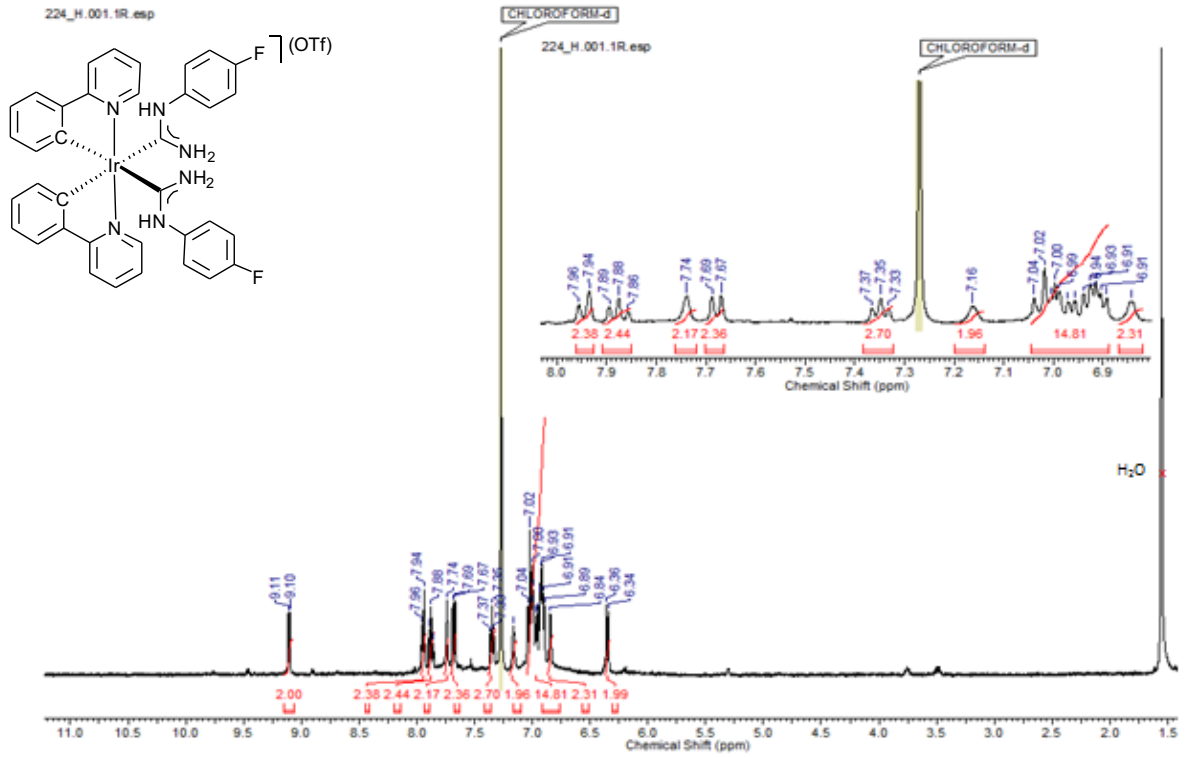

Figure S21. ^{1}H NMR spectrum of [**5a**](OTf) in $CDCl_3$

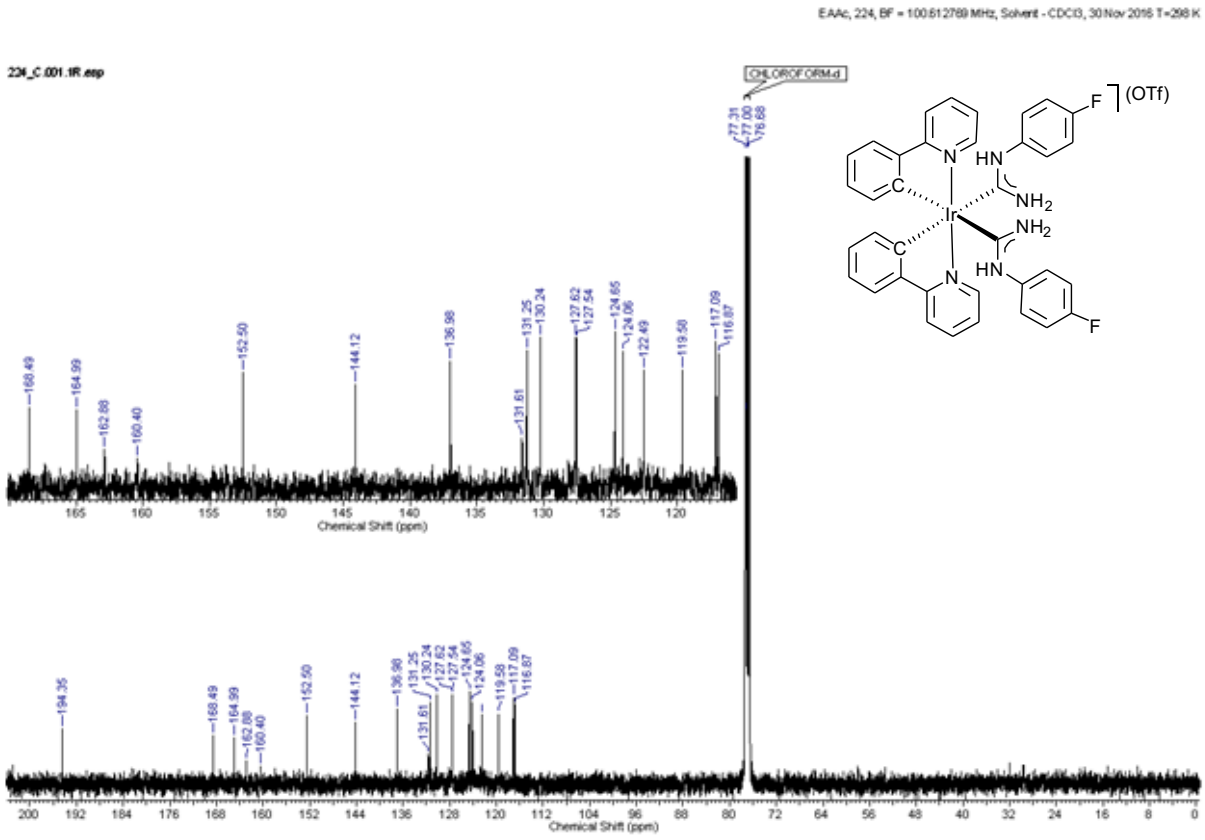

Figure S22. $^{13}C\{^{1}H\}$ NMR spectrum of [**5a**](OTf) in $CDCl_3$

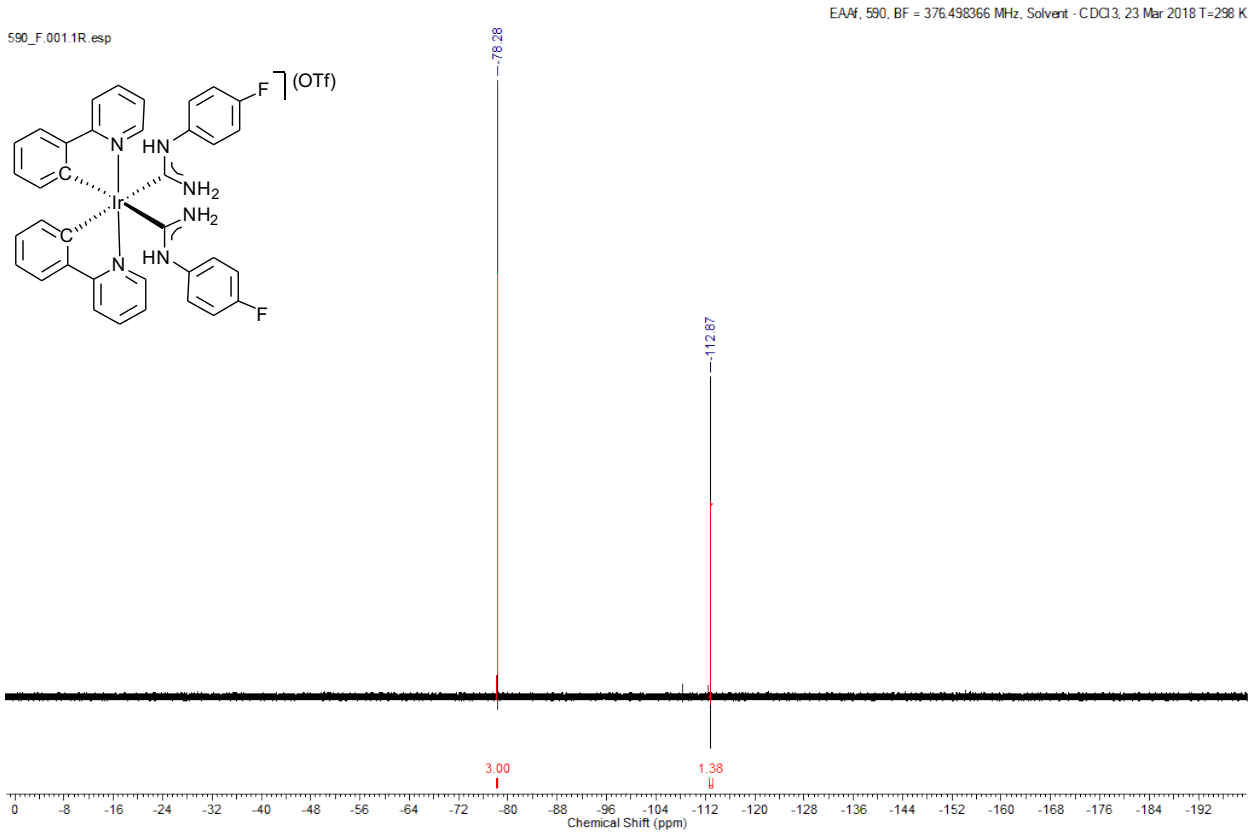

Figure S23. $^{19}F\{^{1}H\}$ NMR spectrum of [**5a**](OTf) in $CDCl_3$

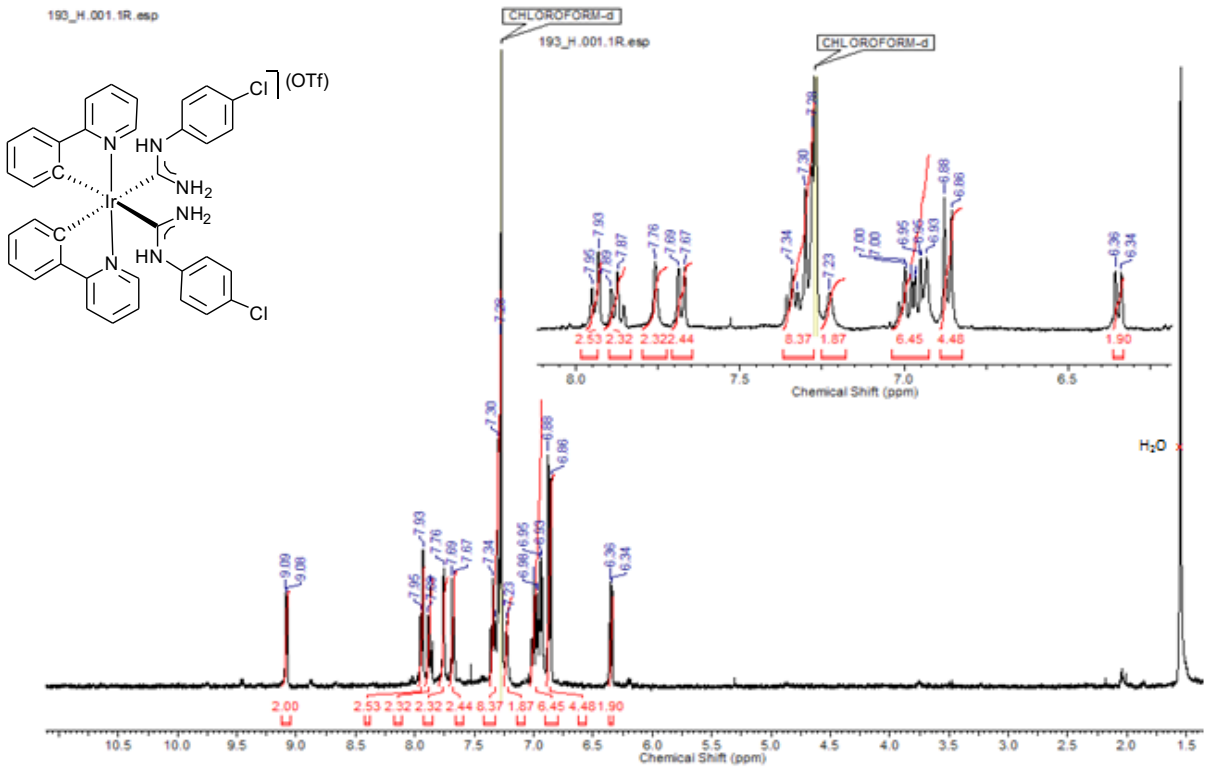

Figure S24. ^{1}H NMR spectrum of [**5b**](OTf) in $CDCl_3$

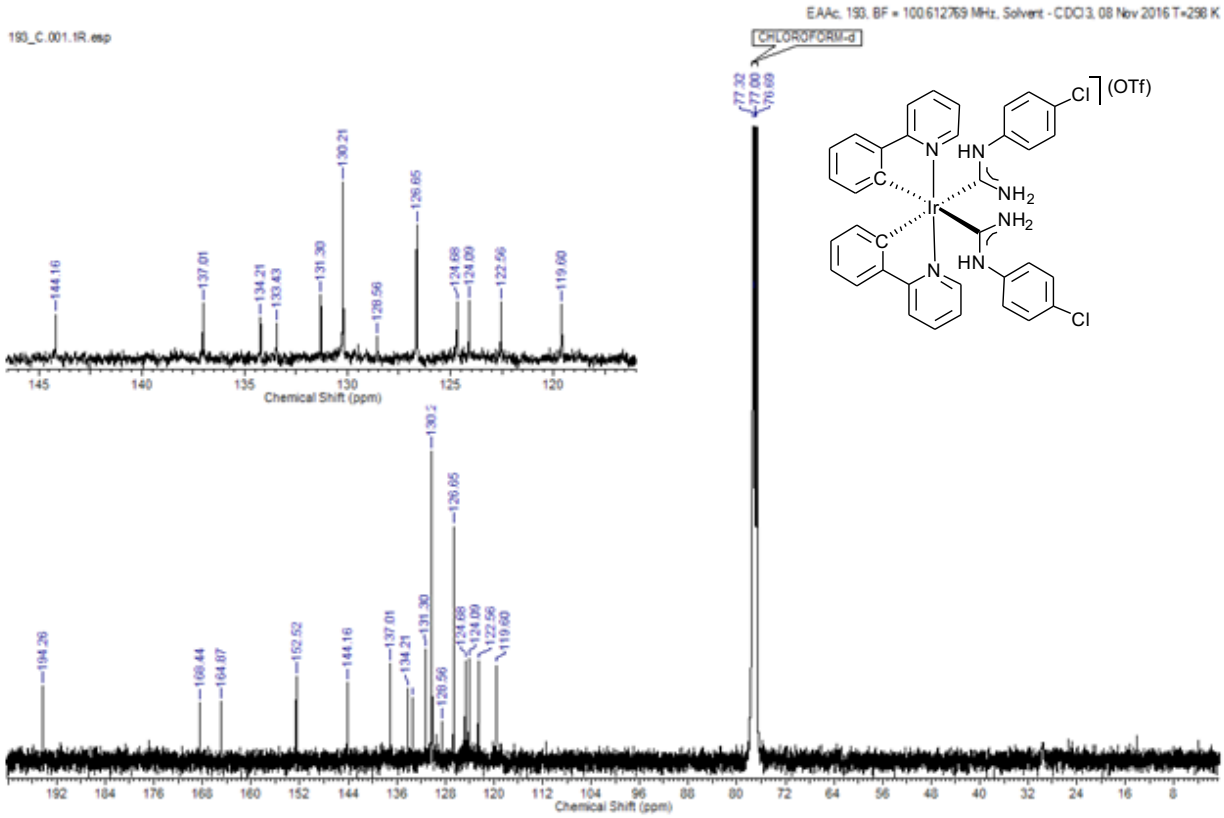

Figure S25. $^{13}C\{^{1}H\}$ NMR spectrum of [**5b**](OTf) in $CDCl_3$

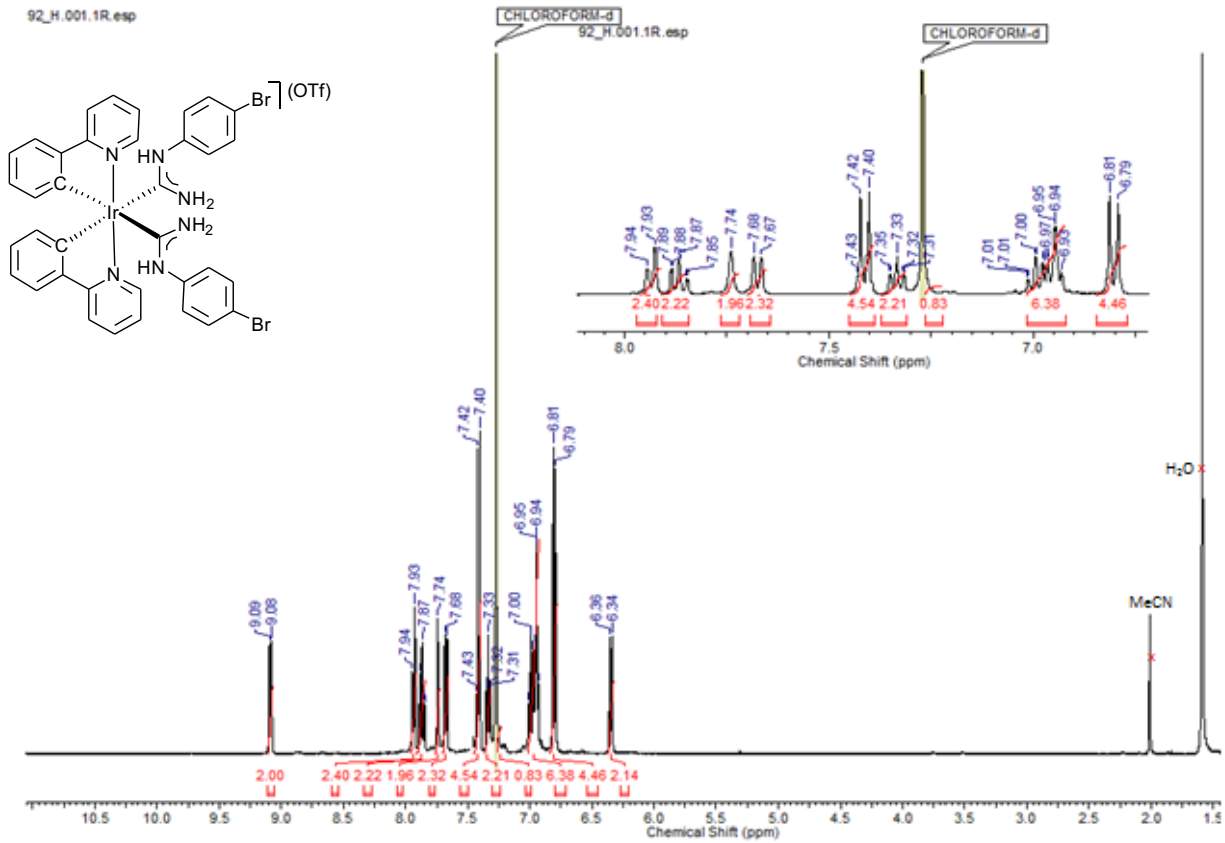

Figure S26. ^{1}H NMR spectrum of [**5c**](OTf) in $CDCl_3$

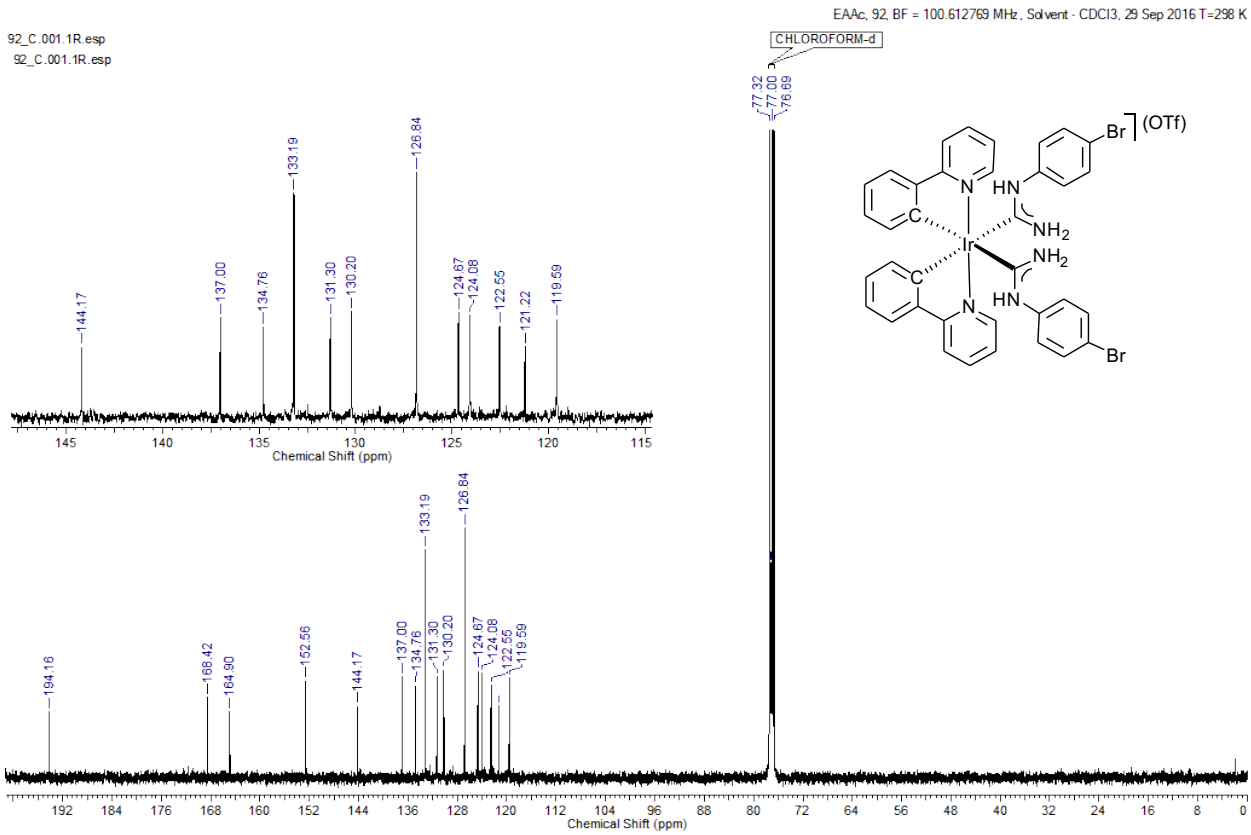

Figure S27. $^{13}C\{^{1}H\}$ NMR spectrum of [**5c**](OTf) in $CDCl_3$

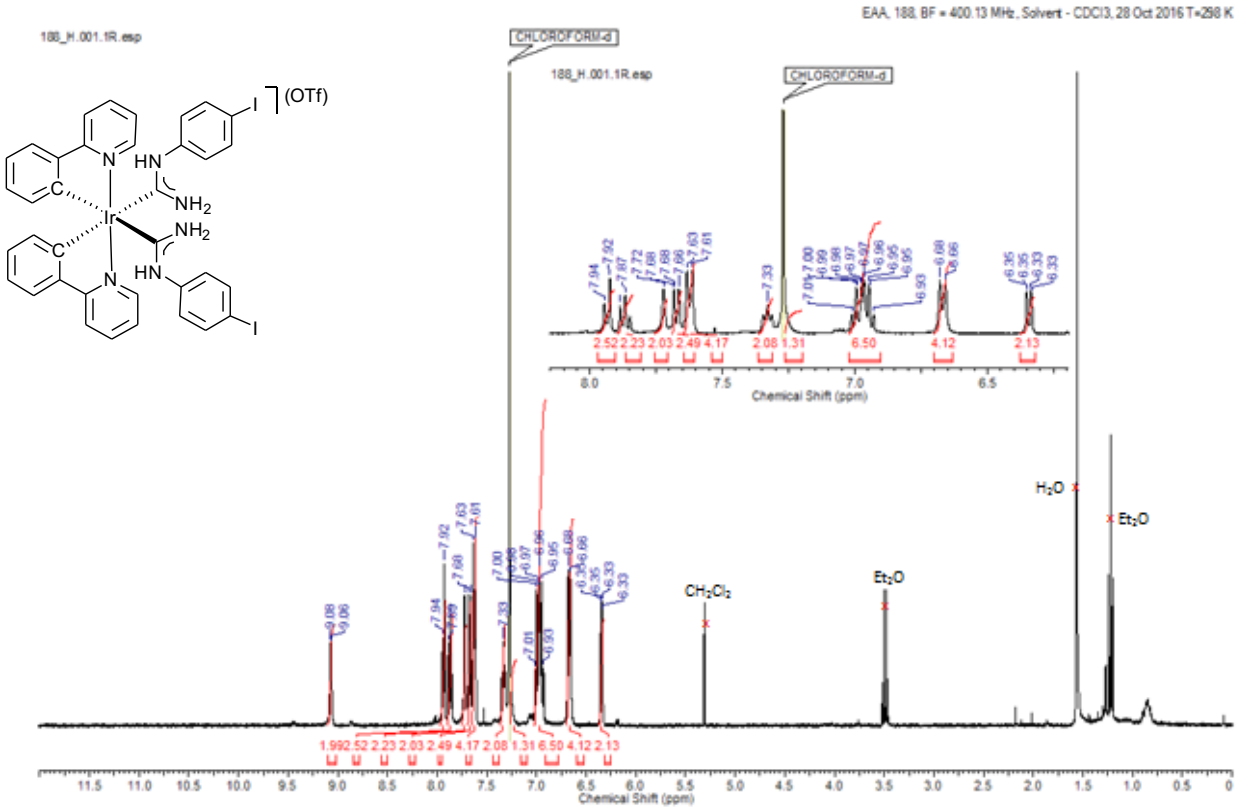

Figure S28. ^{1}H NMR spectrum of [**5d**](OTf) in $CDCl_3$

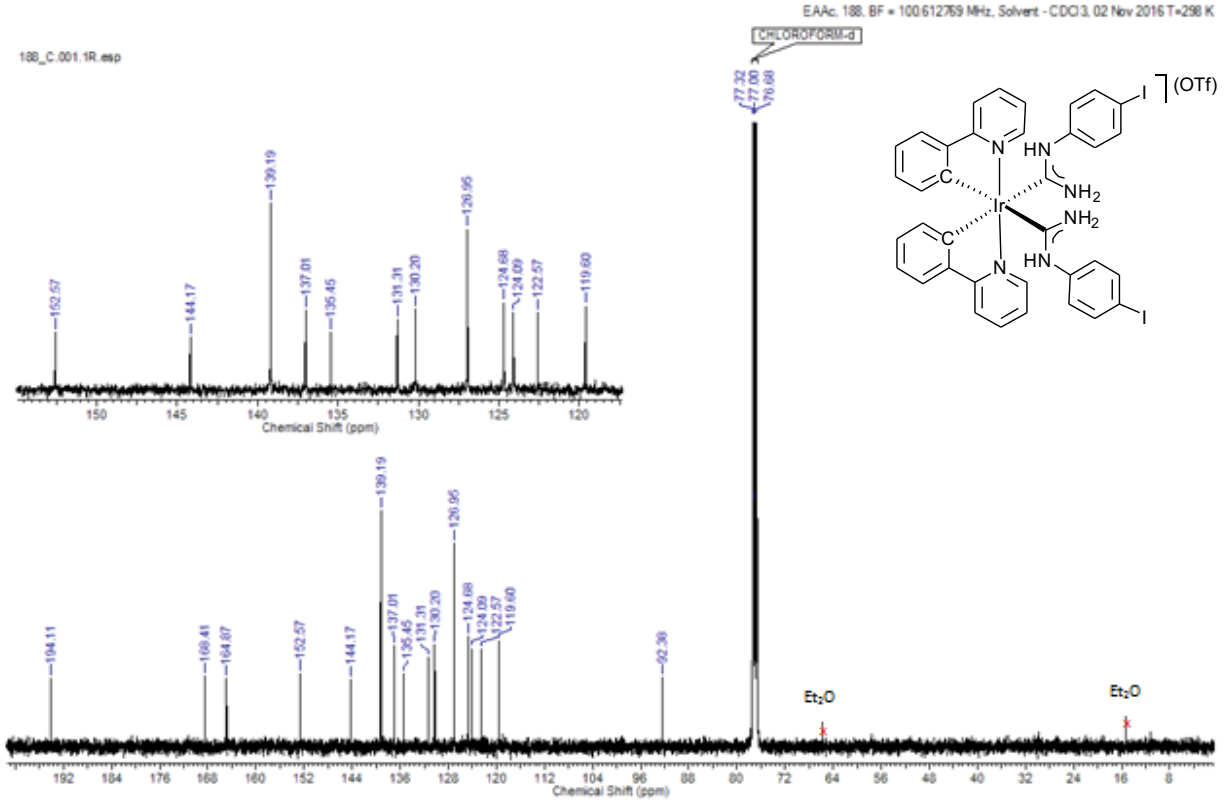

Figure S29. ^{13}C{^{1}H} NMR spectrum of [**5d**](OTf) in $CDCl_3$

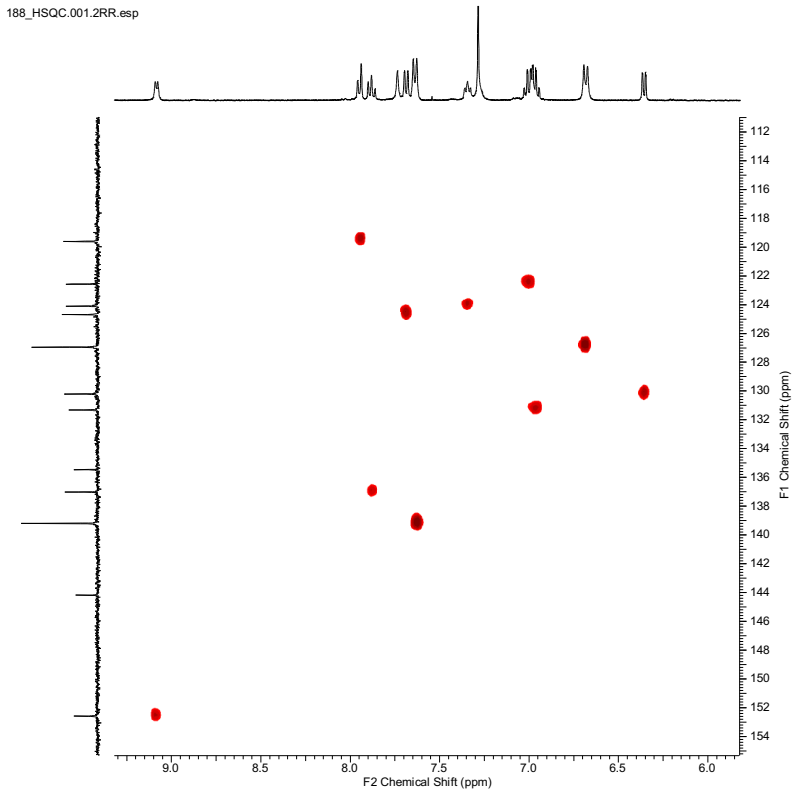

Figure S30. $^{1}H,^{13}C$–HSQC NMR spectrum of [**5d**](OTf) in $CDCl_3$

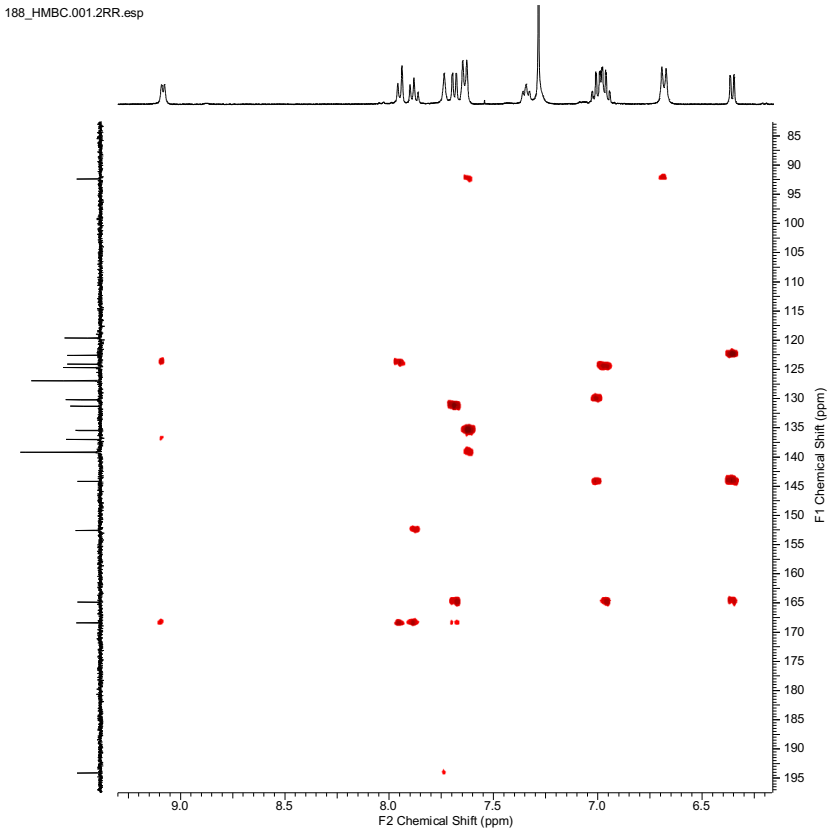

Figure S31. $^{1}H,^{13}C$–HMBC NMR spectrum of [**5d**](OTf) in $CDCl_3$

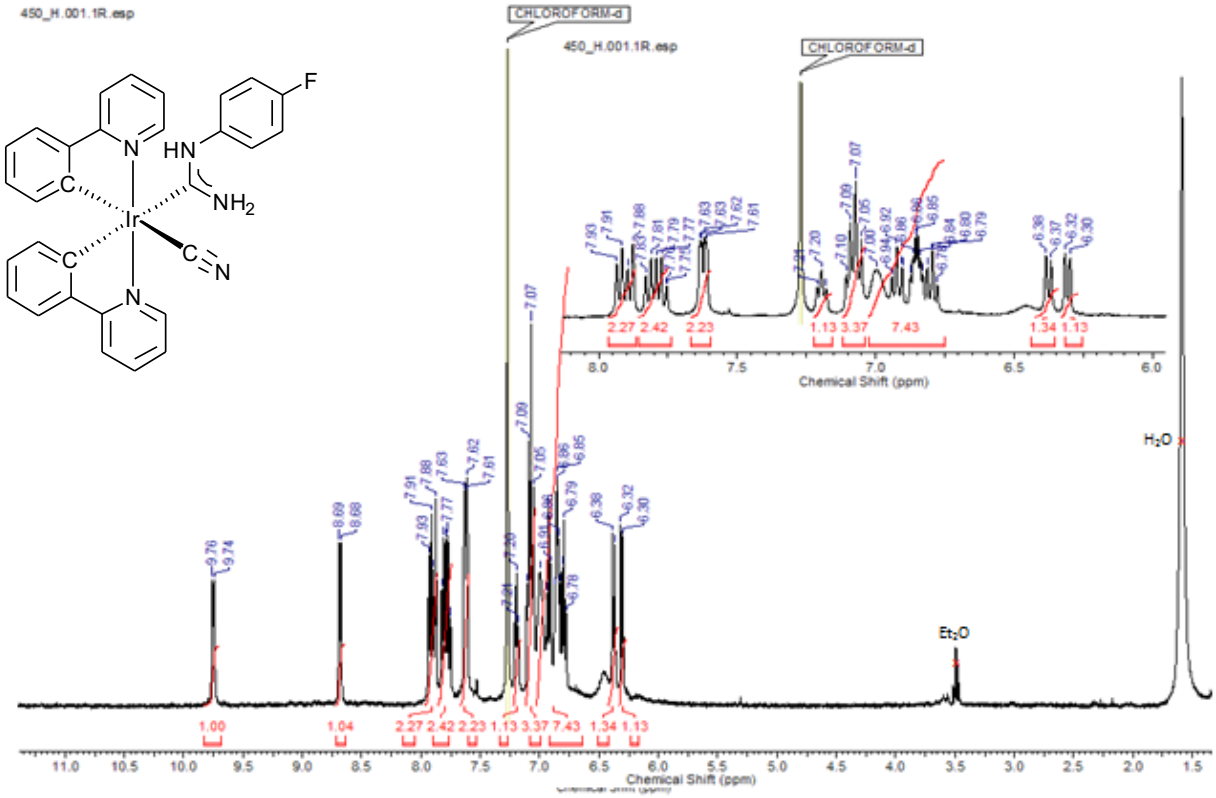

Figure S32. ^{1}H NMR spectrum of **6a** in $CDCl_3$

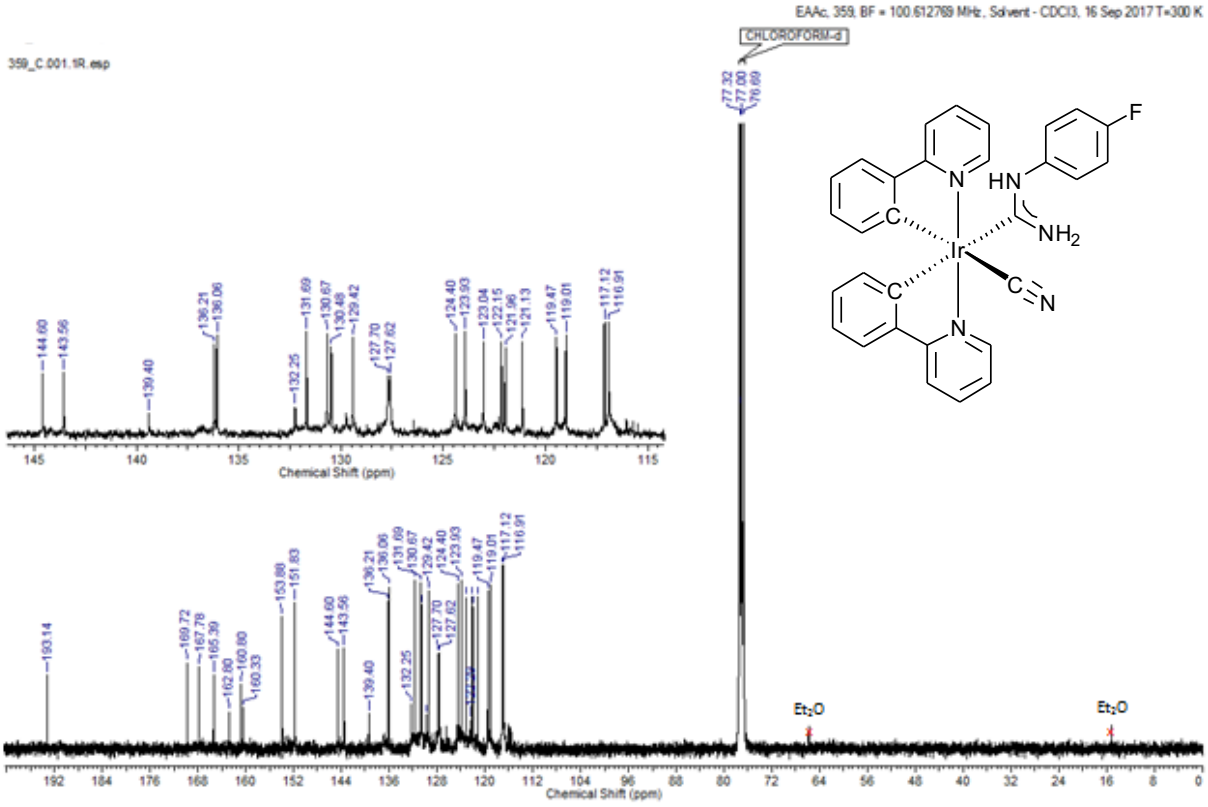

Figure S33. $^{13}C\{^{1}H\}$ NMR spectrum of **6a** in $CDCl_3$

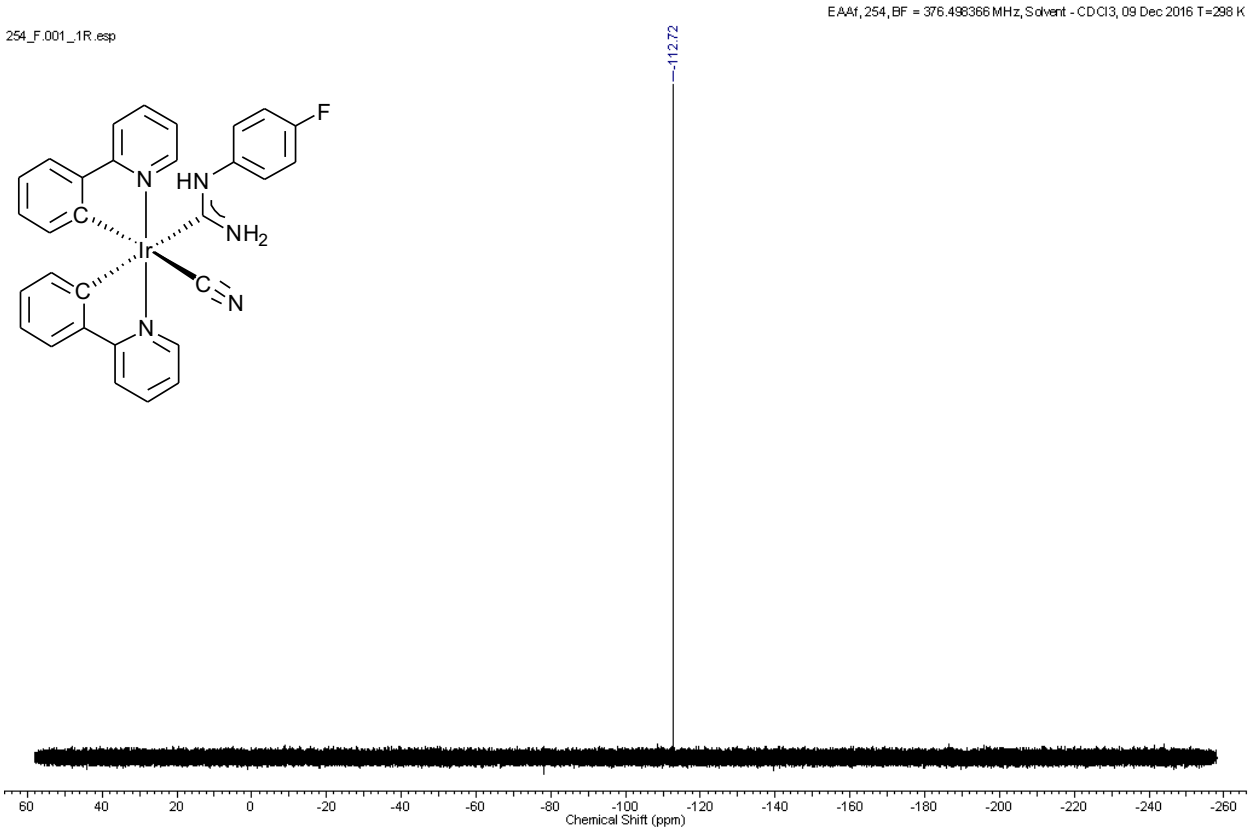

Figure S34. $^{19}F\{^{1}H\}$ NMR spectrum of **6a** in $CDCl_3$

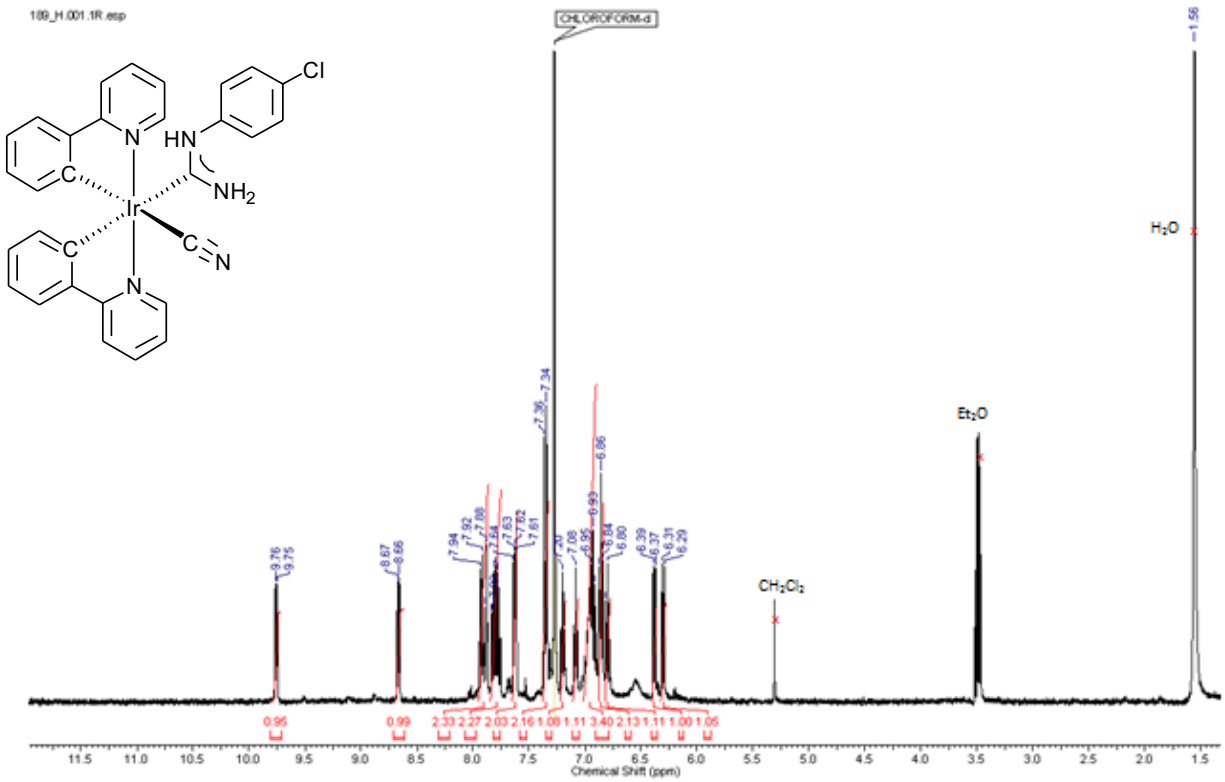

Figure S35. ^{1}H NMR spectrum of **6b** in $CDCl_3$

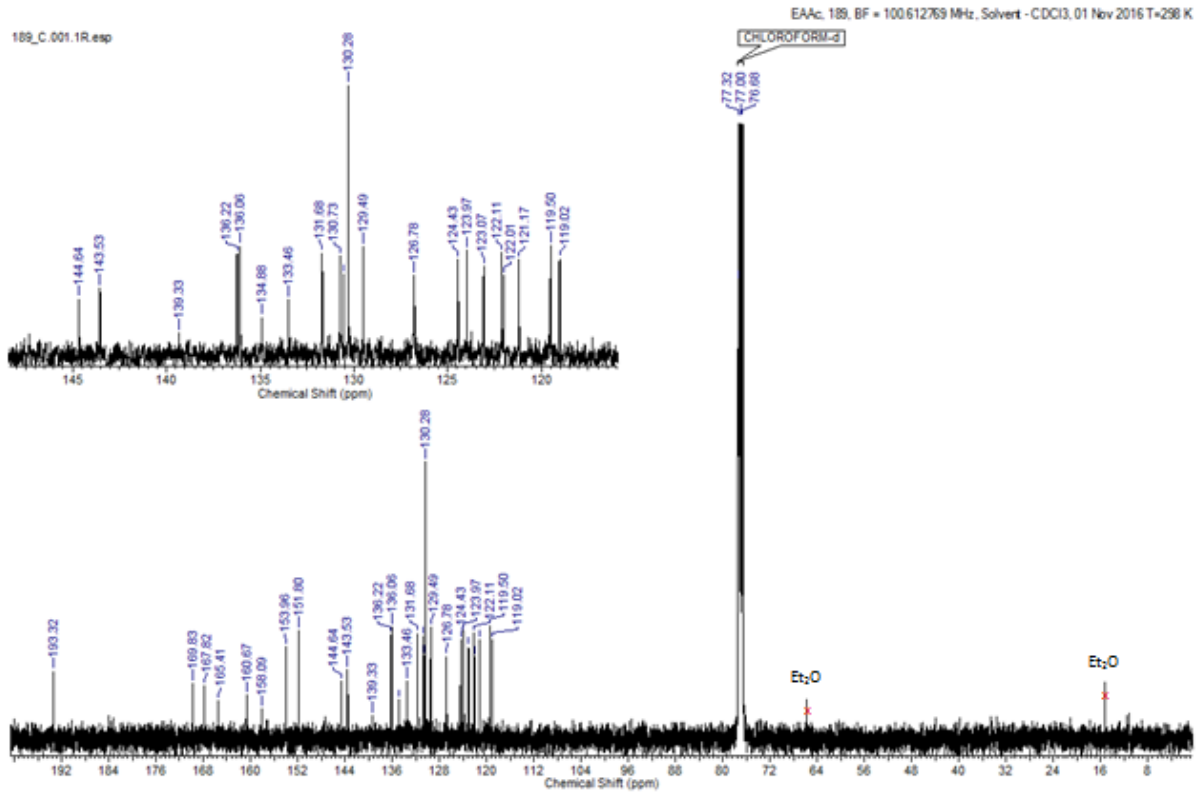

Figure S36. $^{13}C\{^{1}H\}$ NMR spectrum of **6b** in $CDCl_3$

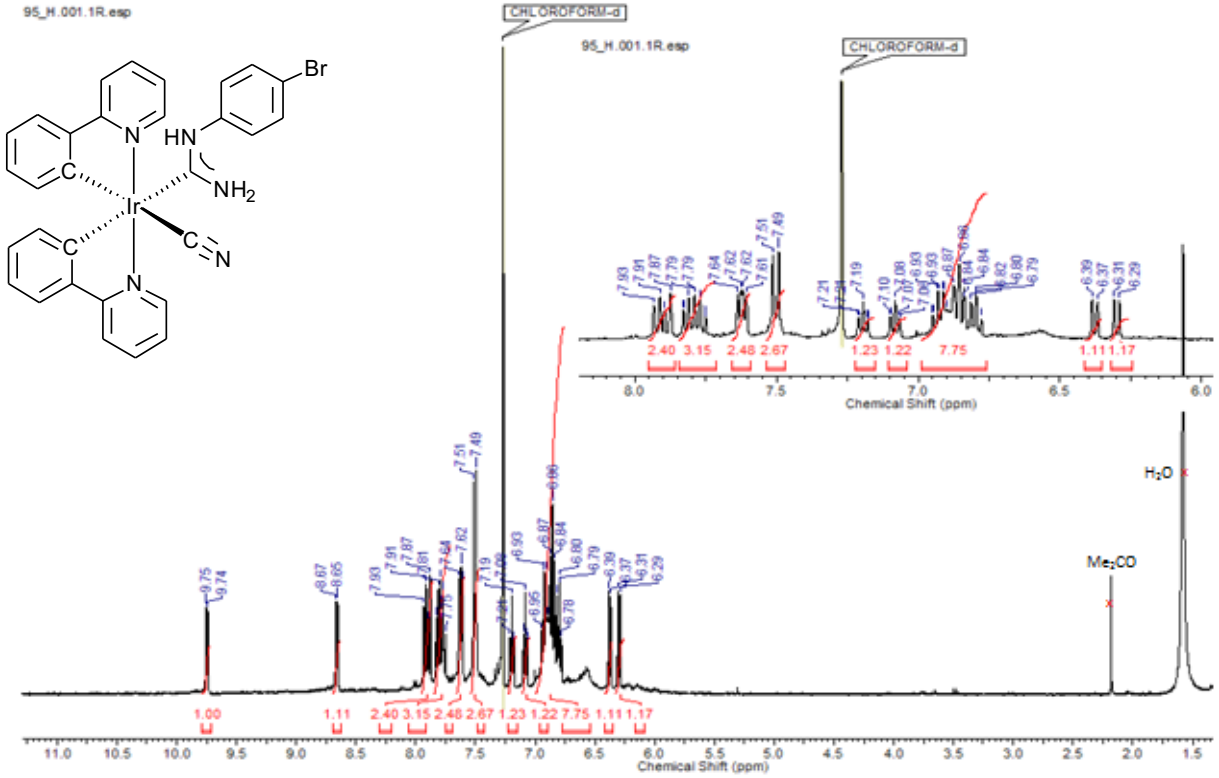

Figure S37. ^{1}H NMR spectrum of **6c** in $CDCl_3$

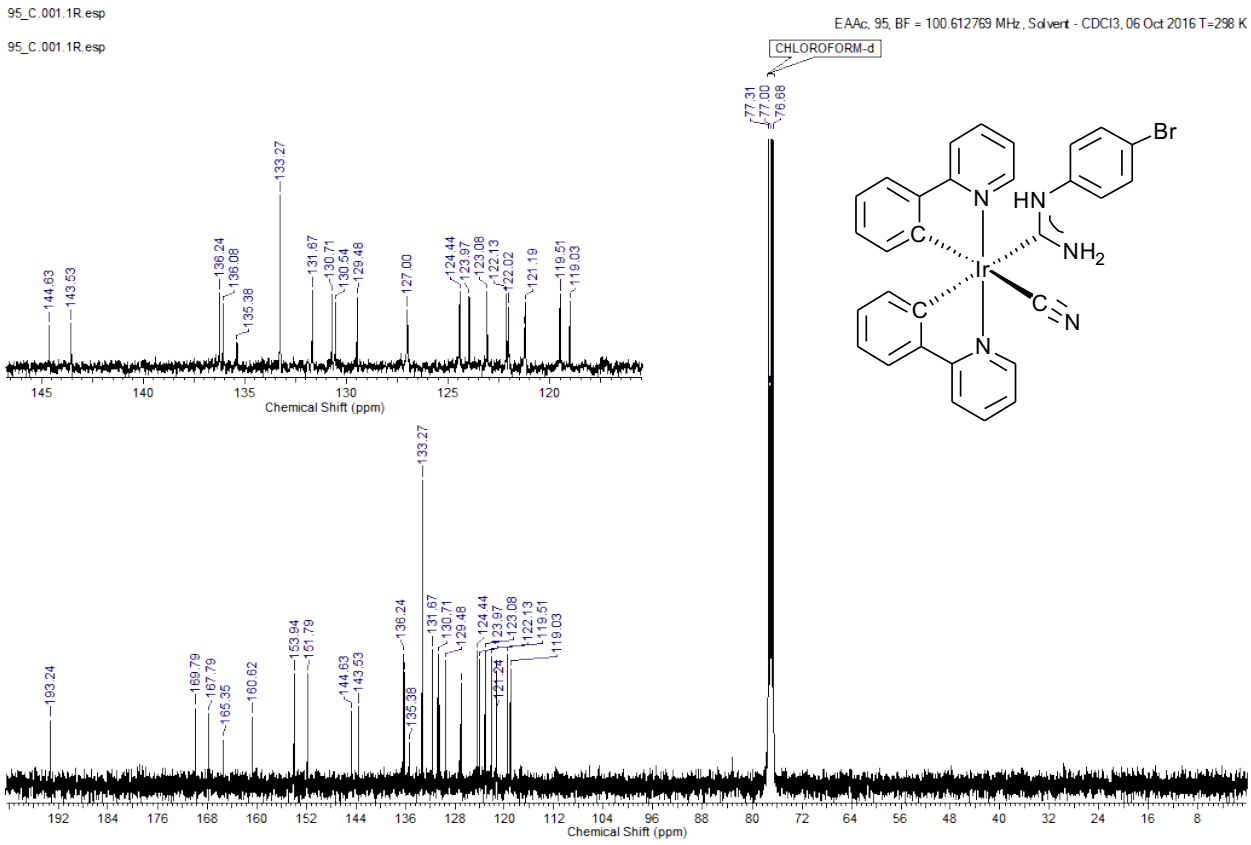

Figure S38. $^{13}C\{^{1}H\}$ NMR spectrum of **6c** in $CDCl_3$

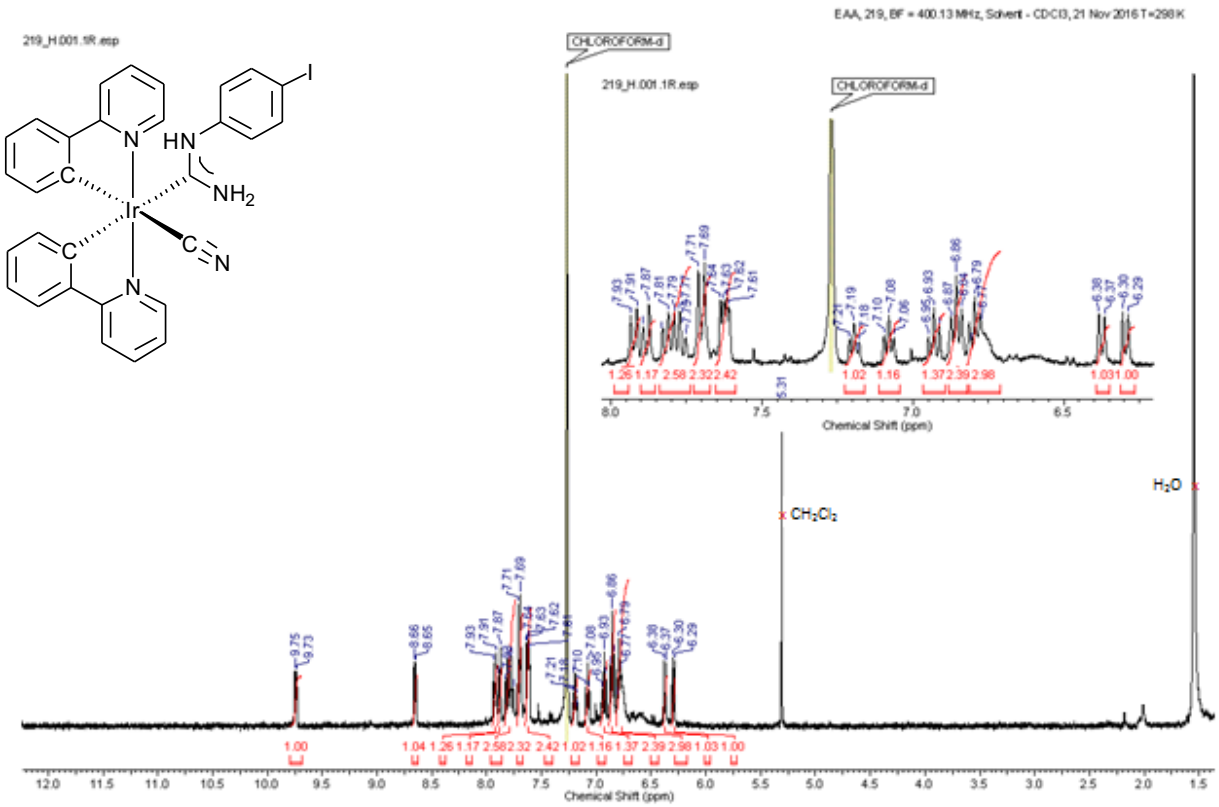

Figure S39. ^{1}H NMR spectrum of **6d** in $CDCl_3$

References

[1] W. J. Geary, *Coord. Chem. Rev.* **1971**, *7*, 81−122.

[2] R. A. Michelin, A. J. L. Pombeiro, M. F. C. Guedes da Silva, *Coord. Chem. Rev.* **2001**, *218*, 75–112.

[3] H. Na, A. Maity, R. Morshed, T. S. Teets, *Organometallics* **2017**, *36*, 2965-2972.

[4] a) M. A. Kinzhalov, V. P. Boyarskiy, K. V. Luzyanin, F. M. Dolgushin, V. Y. Kukushkin, *Dalton Trans.* **2013**, 10394–10397; b) M. A. Kinzhalov, K. V. Luzyanin, V. P. Boyarskiy, M. Haukka, V. Y. Kukushkin, *Organometallics* **2013**, *32*, 5212–5223; c) M. A. Kinzhalov, K. V. Luzyanin, V. P. Boyarskiy, M. Haukka, V. Y. Kukushkin, *Russ Chem Bull* **2013**, *62*, 758–766; d) E. A. Valishina, M. F. C. Guedes da Silva, M. A. Kinzhalov, S. A. Timofeeva, T. M. Buslaeva, M. Haukka, A. J. L. Pombeiro, V. P. Boyarskiy, V. Y. Kukushkin, K. V. Luzyanin, *J. Mol. Catal. A: Chem.* **2014**, *395*, 162−171; e) S. A. Timofeeva, M. A. Kinzhalov, E. A. Valishina, K. V. Luzyanin, V. P. Boyarskiy, T. M. Buslaeva, M. Haukka, V. Y. Kukushkin, *J. Catal.* **2015**, *329*, 449−456; f) T. B. Anisimova, M. A. Kinzhalov, M. F. C. Guedes da Silva, A. S. Novikov, V. Y. Kukushkin, A. J. L. Pombeiro, K. V. Luzyanin, *New J. Chem.* **2017**, *41*, 3246–3250.

[5] S.-W. Lai, M. C.-W. Chan, K.-K. Cheung, C.-M. Che, *Organometallics* **1999**, *18*, 3327-3336.

[6] M. K. Nazeeruddin, R. Humphry-Baker, D. Berner, S. Rivier, L. Zuppiroli, M. Graetzel, *J. Am. Chem. Soc.* **2003**, *125*, 8790-8797.